TKK Dissertations 93
Espoo 2007

MODELLING THE UNBALANCED MAGNETIC PULL IN ECCENTRIC-ROTOR ELECTRICAL MACHINES WITH PARALLEL WINDINGS

Doctoral Dissertation

Andrej Burakov

Helsinki University of Technology
Department of Electrical and Communications Engineering
Laboratory of Electromechanics

TKK Dissertations 93
Espoo 2007

MODELLING THE UNBALANCED MAGNETIC PULL IN ECCENTRIC-ROTOR ELECTRICAL MACHINES WITH PARALLEL WINDINGS

Doctoral Dissertation

Andrej Burakov

Dissertation for the degree of Doctor of Science in Technology to be presented with due permission of the Department of Electrical and Communications Engineering for public examination and debate in Auditorium S1 at Helsinki University of Technology (Espoo, Finland) on the 25th of October, 2007, at 12 noon.

Helsinki University of Technology
Department of Electrical and Communications Engineering
Laboratory of Electromechanics

Teknillinen korkeakoulu
Sähkö- ja tietoliikennetekniikan osasto
Sähkömekaniikan Laboratorio

Distribution:
Helsinki University of Technology
Department of Electrical and Communications Engineering
Laboratory of Electromechanics
P.O. Box 3000
FI - 02015 TKK
FINLAND
URL: http://www.tkk.fi/Units/Electromechanics/
Tel. +358-9-451 2381
Fax +358-9-451 2991
E-mail: andrej.burakov@tkk.fi

ISBN 978-951-22-9005-5
ISBN 978-951-22-9006-2 (PDF)
ISSN 1795-2239
ISSN 1795-4584 (PDF)
URL: http://lib.tkk.fi/Diss/2007/isbn9789512290062/

TKK-DISS-2358

Picaset Oy
Helsinki 2007

ABSTRACT OF DOCTORAL DISSERTATION	HELSINKI UNIVERSITY OF TECHNOLOGY P.O. BOX 1000, FI-02015 TKK http://www.tkk.fi

Author Andrej Burakov

Name of the dissertation

Modelling the unbalanced magnetic pull in eccentric-rotor electrical machines with parallel windings

Manuscript submitted 08.06.2007	Manuscript revised 07.10.2007

Date of the defence 25.10.2007

☐ Monograph	☒ Article dissertation (summary + original articles)

Department	Electrical and Communications Engineering
Laboratory	Electromechanics
Field of research	Electrical machines
Opponent(s)	Dr. David Dorrell
Supervisor	Prof. Antero Arkkio
Instructor	---

Abstract

This research work is focused on developing simple parametric models of the unbalanced magnetic pull produced in eccentric-rotor electrical machines. The influence of currents circulating in the parallel paths of the stator winding on the unbalanced magnetic pull is given the main attention. The interaction between these currents and those circulating in the rotor cage/damper winding is also considered.

First, a parametric force model for an eccentric-rotor salient-pole synchronous machine is developed. The effects of the parallel stator windings are not considered in this model. Next, a low-order parametric force model is built for electrical machines equipped with parallel stator windings but operating without the rotor cage/damper winding. This force model is applicable to salient-pole synchronous machines as well as to induction motors. And finally, a special force model is developed for electrical machines furnished with parallel paths both in the rotor and stator windings. This model accounts for the equalising currents circulating in the rotor and stator windings and also for the interaction between these currents. This third force model can be applied to a salient-pole synchronous machine and to an induction machine. The parameters of the force models are estimated from the results of numerical simulations applying a soft-computing-based estimation program. All the developed force models with the estimated parameters demonstrate a very good performance in a wide whirling frequency range.

The effects of parallel paths in the rotor and stator windings on the unbalanced magnetic pull are investigated numerically. The acquired results reveal that the total unbalanced magnetic pull and its constituents related to the fundamental magnetic field and slotting are strongly affected by the presence of parallel paths in the stator winding. However, unlike the rotor cage, parallel stator windings may instigate anisotropy in the unbalanced magnetic pull. In such cases, the results of the numerical impulse response test may differ significantly from the conventional calculation results. It is also shown that, despite the fact that the number of parallel paths in the stator is often substantially lower than the number of parallel paths in the rotor, parallel stator windings may still provide a more efficient UMP mitigation than the rotor cage/damper winding..

Keywords parallel windings, rotor eccentricity, unbalanced magnetic pull

ISBN (printed) 978-951-22-9005-5	ISSN (printed) 1795-2239
ISBN (pdf) 978-951-22-9006-2	ISSN (pdf) 1795-4584
Language English	Number of pages 154 p.

Publisher Helsinki University of Technology, Laboratory of Electromechanics

Print distribution Helsinki University of Technology, Laboratory of Electromechanics

☒ The dissertation can be read at http://lib.tkk.fi/Diss/2007/isbn9789512290062/

Preface

This research work was conducted in the Laboratory of Electromechanics at Helsinki University of Technology.

I gratefully acknowledge the invaluable help, guidance and support received throughout the whole course of this project from Professor Antero Arkkio. For discovering the potential in me and maintaining the fruitful and encouraging discussions, I owe my sincere gratitude to Professor Asko Niemenmaa (Head of the Laboratory) and Emeritus Professor Tapani Jokinen. I am thankful to Dr. Asmo Tenhunen and Dr. Timo Holopainen for sharing their profound experience and knowledge of electrical machines with me. I am much obliged to Mr. Ari Haavisto for his invaluable help and assistance in practical matters. I remain grateful to Mrs. Marika Schröder, who helped me in mastering the bureaucratic impediments. I am also greatly indebted to my colleagues and friends who made it possible to keep my spirits high all the way through my postgraduate studies.

It is impossible to overestimate the favourable stimulus I experienced sharing my life with Mr. Gábor Gyöngy. The steal-solid support, relentless encouragement and unsurpassed enthusiasm always showed by Mr. Vasil Denchev is also very much appreciated. Dr. Marian Dumitru Negrea is gratefully acknowledged for his thoughtful and attentive advice.

I would like to express heartfelt gratitude to my deceased grandparents Zinaida and Andrej Fitingovs for their invaluable contribution to developing my personality. My dearly-loved parents are thankfully acknowledged for their kindness, dedication and strong belief in me throughout all my life. I also owe great gratitude to my dearest brothers and sister.

For teaching me to conquer the most difficult challenges, I am genuinely obliged to my close friend, Mr. Aleksandr Miteniov “Mituxa”.

My deepest gratitude I reserve for my beloved wife Marija, for being a vital source of inspiration, encouragement and happiness. It is her patience, love and devotion that made it possible to successfully complete this Dissertation and I wholeheartedly dedicate it to her.

The continuous financial support from the Graduate School in Electrical Engineering is acknowledged gratefully. I also highly appreciate the financial aid granted by Emil Aaltosen Foundation.

Espoo, May 2007

Andrej Burakov

Content

List of publications

The thesis consists of an overview and the following publications:

P1. Burakov, A., Tenhunen, A., Arkkio, A. 2005. Applying Genetic Algorithms to identify the parameters of a low-order force model for a salient-pole synchronous machine with eccentric rotor. *8-th International Conference on Modeling and Simulation of Electric Machines, Converters and Systems*, April 17-20, 2005, Hammamet, Tunisia, 5 p.

P2. Burakov, A., Arkkio, A. 2006. Low-order parametric force model for a salient-pole synchronous machine with eccentric rotor. *Electrical Engineering (Archiv fur Elektrotechnik)*, Springer Berlin / Heidelberg, Vol. 89, No. 2, pp. 127-136.

P3. Burakov, A., Arkkio, A. 2006. Low-order parametric force model for eccentric-rotor electrical machine with parallel connections in stator winding. *IEE Proceedings, Electric Power Applications*, Vol. 153, Issue 4, pp. 592-600.

P4. Burakov, A., Arkkio, A. 2006. Validity of numerical impulse response test in studying unbalanced magnetic pull in electrical machines with parallel stator windings. *Proceedings of XVII International Conference on Electrical Machines*, September 2-5, 2006, Chania, Crete Island, Greece, 5 p.

P5. Burakov, A., Arkkio, A. 2007. Low-order parametric force model for eccentric-rotor electrical machine equipped with parallel stator windings and rotor cage. *IET Electric Power Applications*, Vol. 1, Issue 4, pp. 532-542.

P6. Burakov, A., Arkkio, A. 2007. Mitigation of UMP components by the parallel stator windings in eccentric-rotor electrical machines. *The IEEE International Electric Machines and Drives Conference (IEMDC 2007)*, May 3-5, 2007, Antalya, Turkey, pp. 1638-1642.

P7 Burakov, A., Arkkio, A. 2007. Comparison of the unbalanced magnetic pull mitigation by the parallel paths in the stator and rotor windings. *IEEE Transactions on Magnetics*, in press.

List of symbols and abbreviations

Symbols used and their SI units of measure

Symbols in **bold** represent vector quantities, symbols in *italic* represent scalar quantities, underlined quantities are complex-valued.

0’	rotor axis, [-]
A	magnetic vector potential, [Wb/m]
A_{p-1}, A_{p+1}	force model parameters, [H]
B	magnetic flux density, [T]
B	total magnetic flux density, [T]
$B_{p,1}$	first constituent of the fundamental magnetic flux density component caused by interaction of the fundamental MMF waves with constant permeance term, [T]
$B_{p,2}$	second constituent of the fundamental magnetic flux density component caused by interaction of the fundamental MMF waves with the first Fourier series component of the air gap permeance related to rotor saliency, [T]
B_n	magnetic flux density component normal to the surface, [T]
B_t	magnetic flux density component tangential to the surface, [T]
B_x	magnetic flux density component in *x*-direction, [T]
B_y	magnetic flux density component in *y*-direction, [T]
B_z	magnetic flux density component in *z*-direction, [T]
D	electric flux density, [C/m^2]
d_r	outer diameter of the rotor, [m]
E	electric field strength, [V/m]
$\mathbf{e}_z$	unit-vector having *z*-direction, [-]
F	electromagnetic force, [N]
$\underline{F}_\mathrm{e}$	unbalanced magnetic pull, [N]
$\underline{F}_\mathrm{rad}$	radial component of the unbalanced magnetic pull, [N]
$\underline{F}_\mathrm{tan}$	tangential component of the unbalanced magnetic pull, [N]
F_x	electromagnetic force acting along the *x*-axis, [N]

f	force density, [N/m^3]
$\mathbf{G}$	Jacobian matrix
$\mathbf{H}$	magnetic field strength, [A/m]
$\mathbf{J}$	electric current density, [A/m^2]
j	imaginary unit, [-]
$\underline{K}$	frequency response function of the unbalanced magnetic pull, [N/m]
k_0	force model parameter, [N/m]
$k_{\mathrm{cr},\,p\pm1}$	dimensionless coupling factors for $p\pm1$ current harmonics in the rotor winding, [-]
$k_{\mathrm{cs},\,p\pm1}$	dimensionless coupling factors for $p\pm1$ current harmonics in the stator winding, [-]
$k_{\mathrm{L,r},\,p\pm1}$	coefficients defining the amounts of the corresponding magnetic flux harmonics that pass through the damper winding from the sources other than rotor currents, [H]
$k_{\mathrm{L,s},\,p\pm1}$	coefficients defining the amounts of the corresponding magnetic flux harmonics that pass through the stator winding from the sources other than stator currents, [H]
k_{p-1}, k_{p+1}	force model parameters, [N·rad/(m·s)]
$L_{\mathrm{r},\,p\pm1}$	inductances of the damper winding for $p\pm1$ magnetic flux density harmonics, [H]
$L_{\mathrm{s},\,p\pm1}$	inductances of the stator winding for $p\pm1$ magnetic flux density harmonics, [H]
l_{e}	effective air-gap length, [m]
m	wave number, [-]
$\mathbf{n}$	unit-vector normal to the surface, [-]
n	wave number, [-]
$R_{\mathrm{r},\,p\pm1}$	resistances of the damper winding for $p\pm1$ current harmonics, [Ω]
$R_{\mathrm{s},\,p\pm1}$	resistances of the stator winding for $p\pm1$ current harmonics, [Ω]
r	radius of the integration surface, [m]
r_{r}	inner radius of the air gap, [m]

r_s	outer radius of the air gap, [m]
S	area of the integration surface, [m^2]
S_{ag}	area of the air gap cross section, [m^2]
$\underline{S}_{r,p\pm1,1}$, $\underline{S}_{r,p\pm1,2}$	force model parameters, [Ω/H]
$\underline{S}_{s,p\pm1,1}$, $\underline{S}_{s,p\pm1,2}$	force model parameters, [Ω/H]
s	slip of the rotor, [-]
$\mathbf{t}$	unit-vector tangential to the surface, [-]
t	time, [s]
V	volume of the integration region, [m^3]
W'	magnetic co-energy, [J]
$\underline{z}_{p-1}$, $\underline{z}_{p+1}$	force model parameters, [rad/s]
δ_0	nominal air gap, [m]
$\underline{\delta}_{ecc}$	rotor eccentricity, [m]
ε	permittivity, [F/m]
ϕ	reduced electric scalar potential, [V]
φ	angular coordinate, [rad]
$\varphi_{ecc.0}$	initial phase angle of the rotor eccentricity, [rad]
φ_p	phase angle between the fundamental magnetic flux density component and the fundamental MMF vector of the field winding, [rad]
μ	permeability, [H/m]
μ_0	permeability of free space, [H/m]
ν	reluctivity, [m/H]
ρ	electric charge density, [C/m^3]
σ	conductivity, [S/m]
τ	Maxwell stress tensor, [N/m^2]
ω_1	angular frequency of the supply voltage, [rad/s]
ω_{ecc}	whirling angular velocity, [rad/s]
ω_{ecc}^{r}	whirling angular velocity in rotor frame of reference, [rad/s]
Ω	mechanical angular velocity of the rotor, [rad/s]

ψ	magnetic scalar potential, [Wb·m]
x^*	complex conjugate of x

Abbreviations

2PP	two parallel paths
4PP	four parallel paths
FEA	Finite Element Analysis
FEM	Finite Element Method
FRF	Frequency Response Function
GA	Genetic Algorithms
MMF	Magnetomotive Force
MWFA	Modified Winding Function Approach
UMP	Unbalanced Magnetic Pull
WFA	Winding Function Approach

1 Introduction

1.1 Background of the study

In an electrical machine, both radial and tangential electromagnetic forces are generated. However, if the motor is symmetrical with a perfectly centred rotor, the radial electromagnetic forces are cancelled out and the tangential ones produce a rotating torque. In practice, though, due to manufacturing tolerances, wear of bearings, rotor shaft bending and many other factors, the rotor and stator axes hardly ever coincide and, thus, most of the electrical motors operate with some degree of rotor eccentricity.

When the rotor axis does not coincide with the axis of the stator bore, the imbalance of the electromagnetic forces acting between the rotor and stator occurs. Depending on the rotor axis displacement from the stator bore axis and the angular velocity of the eccentric rotor motion, the net electromagnetic force can be significant. Acting roughly in the direction of the shortest air gap, this force, also called ‘Unbalanced Magnetic Pull’ (UMP), tries to further increase the eccentricity magnitude and may cause serious damage to the electrical machine.

There are several different types of eccentric rotor motion (also called ‘rotor whirling’). One common eccentricity form is cylindrical circular rotor whirling. It implies that the rotor axis, when displaced from the stator bore axis, remains always parallel to the latter and travels around it in a circular orbit with a certain radius (called ‘whirling radius’) and a certain angular velocity (called ‘whirling angular velocity’). The cross section of an electrical motor operated with the cylindrical circular rotor eccentricity is shown in Figure 1.1. Two special cases of cylindrical circular whirling are frequently mentioned in scientific literature. These are static and dynamic eccentricity. The former occurs when the eccentric rotor displacement remains stationary with respect to the stator, i.e. the whirling angular velocity is zero ($\omega_{\mathrm{ecc}} = 0$). Dynamic eccentricity implies that the whirling angular velocity is the same as the mechanical angular velocity of the rotor ($\omega_{\mathrm{ecc}} = \Omega$).

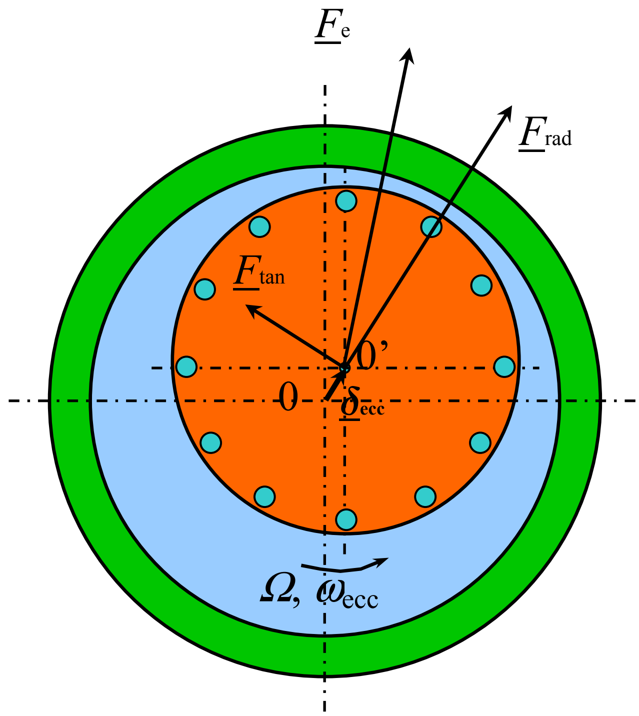

Figure 1.1 Cross section of electrical machine with eccentric rotor.

Rotor eccentricity originates an additional permeance wave, which has two poles. This permeance wave, by interacting with the existing Magnetomotive Force (MMF) harmonics, generates magnetic field harmonics, the orders of which differ by ± 1 from the orders of the corresponding MMF harmonics. These so-called 'eccentricity harmonics' disturb the symmetric distribution of the magnetic field and infringe the equilibrium of the electromagnetic forces acting upon the rotor. As a result, the UMP occurs. The UMP is calculated by integrating the squared magnetic flux density over the whole circumferential length of the machine

$$\underline{F}_e = \frac{d_r l_e}{4\mu_0} \int_0^{2\pi} B^2(\varphi)\, e^{j\varphi}\, d\varphi \tag{1.1}$$

here, d_r is outer diameter of the rotor; l_e is effective air-gap length of the electrical machine; μ_0 is permeability of a free space; φ is angular coordinate; j is imaginary unit.

Equation (1.1) is a simplified form of the complete expression for the total electromagnetic force calculation, which is presented later in Chapter 2. In Eq. (1.1), the magnetic field is assumed to consist entirely of the radial component, which crosses the air gap in radial direction, whereas the tangential magnetic field component is neglected.

Note that B, in Eq. (1.1), is the total magnetic flux density containing all the harmonics. The UMP is assumed to be generated due to the interaction of two magnetic flux density harmonics

$$\underline{F}_{\mathrm{e}} = \frac{d_{\mathrm{r}} l_{\mathrm{e}}}{4\mu_0} \int_0^{2\pi} \left(\sum_{-\infty}^{\infty} \sum_{-\infty}^{\infty} \underline{B}_m \underline{B}_n^{\,*} \right) \mathrm{e}^{\mathrm{j}(m-n+1)\varphi} \mathrm{d}\varphi \tag{1.2}$$

here, m and n denote the wave numbers of the magnetic flux density harmonics, the asterisk denotes the complex conjugate; the underlined quantities are complex-valued.

Equation (1.2) shows that a net non-zero UMP can only be produced by the magnetic flux density components with wave numbers satisfying the condition $m - n = \pm 1$. As explained earlier, the rotor eccentricity causes additional magnetic field harmonics with wave numbers differing by ± 1 from the orders of the magnetic field components that exist in a machine with a concentric rotor. Interaction between these original harmonics and those produced by the rotor eccentricity is the source of the UMP.

Vibrations associated with the UMP develop excessive stress on the rotor bearings, deteriorate the performance and reduce the critical speed and lifetime of the motor. The magnitude and direction of UMP depend on the whirling radius and whirling angular velocity. Besides, the configuration of the stator and rotor windings and the operating point of the machine (supply voltage, load torque, etc.) also considerably influence the UMP.

Magnetic field harmonics caused by the rotor eccentricity induce voltages and, hence, generate currents circulating in the parallel paths of the rotor and stator windings. These currents equalise the magnetic field distribution in the air gap and, by doing so, reduce the resultant UMP.

In electrical motors, the electromagnetic forces are studied by applying analytical or numerical methods. Each of these techniques has its own drawbacks and benefits. By combining the two approaches, it is possible to exploit their advantages (speed and lucidity of the analytical methods and accuracy and flexibility of the numerical methods), while unfettering them from their shortcomings. One example of joining the analytical and numerical techniques is a simple parametric model representing the UMP in eccentric-rotor electrical machines. This force model, derived from the basic equations for electrical motors, with parameters estimated from the results of numerical simulation can be utilised for a quick, yet accurate, calculation of the UMP in a wide whirling frequency range. Alternatively, the model could be used in a coupled electromechanical analysis of the machine, thus providing substantial savings in computation time.

1.2 Aim of the work

The main objective of this study was to develop and verify parametric models for quick and accurate calculation of the electromagnetic force acting between the stator and eccentric rotor. These analytical models were intended not only for induction motors but also for salient-pole synchronous machines. The effects of parallel windings either in the rotor or stator on the UMP were to be accounted for in the models. It was particularly important to model the electromagnetic force in the motor equipped with parallel paths both in the rotor and stator windings. All the models were required to perform accurately in a wide whirling frequency range.

The performance of the force models was to be evaluated using the results of numerical simulations.

This work was also aimed at investigating the interaction between the currents circulating in the parallel paths of the rotor and stator windings.

1.3 Scientific contribution of the work

The most significant scientific contributions of this study are listed below:

1. A parametric force model is developed for an eccentric-rotor salient-pole synchronous machine equipped with a damper winding.
2. A parametric force model is developed for induction and salient-pole synchronous machines equipped with parallel stator windings and operated with rotor eccentricity.
3. A parametric force model is developed for eccentric-rotor induction and salient-pole synchronous machines equipped with parallel stator windings and rotor cage (or damper winding, in the case of a synchronous machine). All the force models exhibited a very good performance in a wide whirling frequency range.
4. The parametric force models are verified using numerical simulations.
5. Parameter estimation programs based on the fusion of soft and hard computing techniques are built. The programs exhibited a fine performance.
6. The limitations of the numerical impulse response test are identified. Means are proposed to improve the accuracy of this method when applied to electromagnetic force calculation in special applications.
7. Knowledge as to how the UMP is affected by the parallel paths in the rotor and stator windings in a wide whirling frequency range is broadened. It is shown

that parallel stator windings considerably suppress the main UMP constituents and, hence, significantly reduce the net UMP. Unlike the parallel paths in the rotor, the parallel stator windings may cause anisotropic UMP behaviour. According to the results of numerical analysis, parallel paths in the stator winding may provide a more efficient UMP mitigation than the rotor cage (damper winding).

8. Comprehension of the interaction between the currents circulating in the parallel paths of the rotor and stator windings is improved. Of particular importance is a new degree of understanding of how the UMP is influenced by this interaction.

1.4 Structure of the work

This dissertation consists of the following major parts:

1. Fundamentals of the electromagnetic field analysis and electromagnetic force calculation are surveyed in Chapter 2. This chapter also presents a comprehensive literature review introducing the evolution of methods for the analysis of eccentric-rotor electrical machines. The state-of-the-art of the techniques for electromagnetic force calculation is also provided.
2. One of the developed force models is presented in Chapter 3, in which parameter estimation is also discussed briefly.
3. The main results acquired over the course of this work are presented and discussed in Chapter 4.
4. In Chapter 5, the accomplished work and main results are summarised concisely.

Chapters 3 and 4 are based on the author's publications, which are reprinted at the end of this dissertation and constitute its final part.

Publication P1

In this paper, a simple parametric force model is applied to describe the UMP acting on the eccentric rotor of a salient-pole synchronous machine. The force model was originally developed and used for a cage induction machine.

This publication also introduces a new parameter estimation technique, which is based on the fusion of soft computing and hard computing methods. The soft computing kind of method is represented by Genetic Algorithms (GA), whereas, the method of least squares represents the hard computing techniques. By combining the two approaches, the unknown force model parameters are estimated very quickly from the results of numerical calculation. The force model with the acquired parameter values demonstrates a very good performance.

The main benefits of the parameter estimation technique presented are:

1. fast acquisition of the unknown parameters. This advantage becomes especially apparent when the number of unknown parameters (the dimensionality of the search space) increases;
2. global optimum point can be detected in the multimodal (containing numerous local optima) landscapes.

The parameter estimation technique developed was later successfully tested on more complicated problems (force models containing many more unknown parameters) and proved to perform very well, even when some other estimation techniques failed.

The paper has been written by Andrej Burakov. He has also developed and tested the parameter estimation procedure. The finite element model and the force model were developed by Professor Antero Arkkio (Arkkio et al., 2000), the supervisor of the thesis. Asmo Tenhunen provided help with numerical calculations of the electrical machine. Antero Arkkio and Asmo Tenhunen also contributed to this work through their valuable comments and discussions.

Publication P2

A theoretical analysis of the magnetic field in a salient-pole synchronous machine with eccentric rotor is carried out in this paper. The operation of the machine in a wide whirling frequency range is considered. The influence of the currents circulating in the parallel paths of the damper winding on the UMP is the main topic of this study. The investigation is based on the classical two-axis approach and permeance harmonic analysis.

As a result of this study, a low-order parametric force model for an eccentric-rotor salient-pole synchronous machine is developed. The force model, with parameters estimated from the results of numerical calculations, performs very well in the whole whirling frequency range studied ([–100, 100] Hz).

A numerical impulse response test was applied to calculate the electromagnetic forces on the whirling rotor. These results were compared with the results from the conventional numerical calculation technique (forced whirling method) and yielded a very good agreement. Thus, the suitability of the computationally efficient impulse response test for the UMP analysis in a salient-pole synchronous machine was verified.

The paper has been written by Andrej Burakov. The force model presented in the publication is designed by Andrej Burakov. Professor Antero Arkkio contributed to this work through his valuable comments and discussions. He also developed the finite element model of the electrical machine.

Publication P3

Parallel stator windings have been long known for their beneficial effects on the UMP. Nowadays, parallel stator windings are commonly used in electrical motors, as they ensure a lower level of vibration and noise emitted by the machine. Moreover, parallel connections also simplify the manufacturing of the stator winding in large electrical machines.

In this publication, the influence of parallel stator windings on the UMP is investigated. A simple low-order parametric model to represent the eccentricity force acting in a salient-pole synchronous machine is developed and verified. The force model is designed for a machine equipped with parallel stator windings and is capable of accurately describing the UMP in a wide whirling frequency range. A classical permeance harmonic theory is applied in this work. Despite the rotor saliency, a vector representation is utilised in this study, instead of resorting to a conventional two-axis approach.

The parameters of the developed force model are estimated from the results of numerical impulse response test. A very accurate performance of the model is observed throughout the whole whirling frequency range studied. The presented force model, without modifications to its original expression, is also applied to an induction motor with parallel stator windings. Again, a very good performance is recorded.

The paper has been written by Andrej Burakov. The force model is designed by Andrej Burakov. Professor Antero Arkkio contributed to this work through his valuable comments and discussions. He also built the finite element model of the electrical machines involved in this study.

Publication P4

In recent years, the numerical impulse response test has been successfully applied for the calculation of electromagnetic forces, rotor cage currents and magnetic flux density harmonics in electrical machines. The results acquired using this approach usually provided a fairly good agreement with the results from the traditionally used forced whirling method. The major benefit of using the impulse response test instead of the forced whirling method is a significant reduction of computation time. The savings in computation time can be as much as 95%.

However, in certain applications, the results from the numerical impulse response test may differ substantially from the results provided by the traditional computation methods. This poses a question as to the appropriateness of the impulse response test for such problems. These difficulties are particularly pertinent to the UMP analysis in electrical machines equipped with parallel stator windings, which may render the electromagnetic system of electrical machine anisotropic.

In this publication, the performance of the numerical impulse response test applied to the UMP calculation in an induction motor with parallel stator windings is investigated. Different combinations of the stator and rotor winding layouts are studied. Some procedures to improve the accuracy of the impulse-response-test results are put forward. Conclusions as to the applicability of the method for the UMP calculation in electrical machines with parallel windings in the stator are also drawn.

The paper has been written by Andrej Burakov. My co-author, Professor Antero Arkkio, contributed to this work through his valuable comments and expertise in the field of finite-element-calculation techniques.

Publication P5

A rotor eccentricity engenders additional permeance wave in the air gap of an electrical machine. As a result, many new magnetic field harmonics arise, which disturb the symmetric distribution of the magnetic field. The most important of these harmonics are those that have the number of pole-pairs differing by one from the number of pole-pairs of the fundamental field. These are also referred to as “eccentricity harmonics”. When interacting with the fundamental field, the eccentricity harmonics produce the UMP.

Normally, the eccentricity harmonics induce voltages in the parallel circuits of the stator and rotor windings, and, hence, facilitate currents circulating in the windings. The circulating currents can significantly reduce the eccentricity harmonics and the resultant UMP, thus, improving the performance of the electrical machine and extending its lifetime.

In this publication, the electromagnetic force acting on the eccentric rotor of a salient-pole synchronous machine is studied in a wide whirling frequency range. The machine is equipped with parallel stator windings and damper winding. A low-order parametric force model is developed to accurately represent the UMP in the whirling frequency range of interest. The proposed model accounts for the effects of circulating currents on the UMP. Moreover, the interactions between the currents circulating in the stator winding and those in the damper winding are also considered. The force model parameters are estimated from the results of numerical calculation, where the effects of stator and rotor slotting and iron-core saturation are accounted for. The model presented performs fairly well when applied to a salient-pole synchronous machine and to a cage induction motor. Moreover, the force model is also applied to synchronous and induction machines equipped with either parallel stator windings or rotor cage (damper winding). In all these cases, a very good model performance is observed.

The paper has been written by Andrej Burakov. My co-author, Professor Antero Arkkio, has contributed to this work through his valuable comments, discussions and his expertise in the field of finite-element-calculation techniques.

Publication P6

In this publication, the performance of a cage induction motor operated with an eccentric rotor is investigated using Finite Element Method (FEM). A wide whirling frequency range is considered. The main aim of this work is to study the influence of parallel stator windings on the net UMP and UMP components associated with the eccentricity and slot harmonics.

Using Finite Element Analysis (FEA) it is possible to resolve the total electromagnetic force into several constituents, originating from different sources. The UMP component related to the eccentricity harmonics is calculated using the fundamental magnetic field and magnetic flux density harmonics with wave-numbers different by one from the wave-number of the fundamental field. Another UMP constituent, the one associated with rotor and stator slotting, is computed from the magnetic flux density harmonics related to the number of slots in the rotor and stator. The electromagnetic force components are calculated while post-processing the FEA results.

The findings of this work show that the eccentricity and slotting harmonics contribute the most to the total UMP. In the whirling frequency range considered, the UMP constituent associated with the slotting has a very small whirling frequency dependence. Eccentricity harmonics, on the other hand, produce a UMP component that has prominent peaks at certain whirling frequencies. These peaks are also clearly seen in the total UMP.

The parallel stator windings are shown to considerably reduce the net UMP. It is demonstrated that the eccentricity-harmonics-related UMP component is affected the most by the parallel paths, particularly in the whirling frequency range close to the mechanical frequency of the rotor motion. The slotting-related UMP constituent is attenuated almost evenly in the whole whirling frequency range studied. It is also shown that the reduction of the force components related to the eccentricity and slotting harmonics account for the major part of the UMP mitigation by the parallel stator windings.

The paper has been written by Andrej Burakov. My co-author, Professor Antero Arkkio, has contributed to this work through his valuable comments, discussions and his expertise in the field of finite-element-calculation techniques.

Publication P7

The rotor eccentricity introduces additional magnetic field harmonics, which disturb the symmetrical distribution of the magnetic field in the air gap of electrical motors. Because of this asymmetry, the voltages induced in the windings connected in parallel may differ from each other, thus giving rise to the currents circulating in these parallel circuits. The magnetic fields produced by the circulating currents will attenuate the asymmetry of the total magnetic field in the air gap and, as a result, reduce the UMP.

It is well known that parallel circuits in the rotor and stator windings effectively reduce the UMP magnitude. Numerous contributions to this topic can be found in scientific literature dating back to the beginning of the 20-th century. However, in the early papers, the authors employed analytical approaches and tried to assess the influence of the parallel windings on the UMP by introducing corresponding coefficients into the electromagnetic force expression. Quite often, the analytical methods could not achieve the desired level of accuracy. Numerical methods were later extensively used in the analysis of electrical motors with rotor eccentricity. However, these studies were mainly concerned with cage induction motors and limited to special cases of static and/or dynamic eccentricity.

In this publication, the results of extensive numerical study on UMP mitigation by the parallel windings in the rotor and stator are presented. Two common types of electrical machine are investigated: cage induction motor and salient-pole synchronous machine. The effects of the rotor cage (damper winding) and parallel stator windings on the eccentricity force are examined in a wide whirling frequency range and compared to each other. The combined influence of parallel windings in the rotor and stator on the UMP is also studied.

The results of this investigation revealed that, depending on the number of parallel circuits, the stator winding may cause uneven UMP reduction on the orthogonal axes. The rotor cage, owing to the large number of parallel paths, attenuated the eccentricity force evenly. Both the test motors equipped with four parallel stator windings experienced lower average UMP level than that recorded for the machines with rotor cage (damper winding) alone. However, as expected, the smallest eccentricity force was produced in the motors incorporating parallel circuits both in the rotor and stator.

The paper has been written by Andrej Burakov. My co-author, Professor Antero Arkkio, has contributed to this work through valuable comments, discussions and his expertise in the field of finite-element-calculation techniques.

2 Overview of the electromagnetic field and force calculation

In this chapter, fundamentals of the electromagnetic field analysis and electromagnetic force calculation are presented. The most common analytical and numerical techniques applied in studying the eccentric-rotor electrical machine are reviewed.

2.1 Electromagnetic field computation

An electrical machine converts mechanical energy into electrical energy and vice versa. This transformation is accomplished through the magnetic field. The interrelationship between the electric field, magnetic field, electric charge and electric current can concisely be expressed by a set of four equations. These evolved through the efforts of several renowned scientists, mainly during the nineteenth century, and were written in their well-known form as differential equations by Maxwell (Silvester and Ferrari, 1996). These governing laws of the electromagnetic field are

$$\nabla \times \mathbf{E} = -\frac{\partial \mathbf{B}}{\partial t} \tag{2.1}$$

$$\nabla \times \mathbf{H} = \mathbf{J} + \frac{\partial \mathbf{D}}{\partial t} \tag{2.2}$$

$$\nabla \cdot \mathbf{D} = \rho \tag{2.3}$$

$$\nabla \cdot \mathbf{B} = 0 \tag{2.4}$$

The constitutive relations describing the material properties are

$$\mathbf{D} = \varepsilon \mathbf{E} \tag{2.5}$$

$$\mathbf{B} = \mu \mathbf{H} \tag{2.6}$$

$$\mathbf{J} = \sigma \mathbf{E} \tag{2.7}$$

Quite often it is more convenient to write Eq. (2.6) using reluctivity $\nu = 1/\mu$ instead of permeability, i.e.

$$\mathbf{H} = \nu \mathbf{B} \tag{2.8}$$

In the equations above, the variables are:

E – electric field strength

H – magnetic field strength

D – electric flux density

B – magnetic flux density

J – electric current density

ρ – electric charge density

ε – permittivity

μ – permeability

ν – reluctivity

σ – conductivity

t – time

Equation (2.1) is Faraday's law of induction; Eq. (2.2) is Ampere's circuital law (with Maxwell's extension accounting for the displacement current $\partial \mathbf{D}/\partial t$); Eq. (2.3) is Gauss's law and Eq. (2.4) is Gauss's law for magnetism. Variables **E**, **H**, **D**, **B**, **J** and ρ may each depend on the space coordinates *x*, *y* and *z* and also time *t*. The quantities ε, μ and σ are not necessarily simple constants, e.g. in ferromagnetic materials, the B-H relationship (Eq. (2.6)) is highly nonlinear. Moreover, in anisotropic materials, the flux density may differ in direction from the corresponding field strength (Luomi, 1993). In such cases, the quantities ε and μ are tensors.

Maxwell's equations, in their complete form, are applied in the calculation of the radiated fields. However, in most electromechanical problems, the electromagnetic wave propagation can be neglected, thus allowing for the displacement current $\partial \mathbf{D}/\partial t$ to be dropped out of Eq. (2.2). Moreover, when good conductors are involved, the current density **J** is significantly larger than the displacement current at all frequencies considered. Thus, a quasi-static approximation of Eq. (2.2) can be used

$$\nabla \times \mathbf{H} = \mathbf{J} \tag{2.9}$$

According to the fundamental result of vector analysis, the divergence of the curl of any twice differentiable vector vanishes identically (Chari and Silvester, 1980). Thus a magnetic vector potential **A** can be introduced,

$$\mathbf{B} = \nabla \times \mathbf{A} \tag{2.10}$$

which satisfies the Maxwell magnetic divergence equation (Eq. (2.4))

$$\nabla \cdot \mathbf{B} = \nabla \cdot (\nabla \times \mathbf{A}) \equiv 0 \tag{2.11}$$

The magnetic vector potential is not completely described by Eq. (2.10), since, according to the Helmholtz theorem of vector analysis, the vector is uniquely defined if, and only if, both its curl and divergence are known, as well as if its value is specified at any point in space. Adding the gradient of any twice-differentiable scalar function ϕ to the vector potential has no effect on the final result, since $\nabla\times(\nabla\phi)\equiv 0$. Because of this arbitrariness, the $\nabla\cdot\mathbf{A}$ can be specified freely. In magnetostatic field problems, the uniqueness of the solution is achieved using the Coulomb gauge

$$\nabla\cdot\mathbf{A}=0 \tag{2.12}$$

The Maxwell electric curl (Eq. (2.1)) can now be written using the magnetic vector potential notation

$$\nabla\times\mathbf{E}=-\frac{\partial}{\partial t}(\nabla\times\mathbf{A})=-\nabla\times\left(\frac{\partial\mathbf{A}}{\partial t}\right) \tag{2.13}$$

This can also be written as

$$\nabla\times\left(\mathbf{E}+\frac{\partial\mathbf{A}}{\partial t}\right)=0 \tag{2.14}$$

Keeping in mind that $\nabla\times(\nabla\phi)\equiv 0$, the result of Eq. (2.14) is

$$\mathbf{E}=-\frac{\partial\mathbf{A}}{\partial t}-\nabla\phi \tag{2.15}$$

here, ϕ is reduced electric scalar potential.

Using the constitutive relation of Eq. (2.7), the current density is given by

$$\mathbf{J}=-\sigma\frac{\partial\mathbf{A}}{\partial t}-\sigma\nabla\phi \tag{2.16}$$

The current density can also be expressed from the Maxwell magnetic curl (Eq. (2.9)) using Eqs. (2.8) and (2.10)

$$\mathbf{J}=\nabla\times(\nu\nabla\times\mathbf{A}) \tag{2.17}$$

Substituting Eq. (2.17) into Eq. (2.16) yields

$$\nabla\times(\nu\nabla\times\mathbf{A})+\sigma\frac{\partial\mathbf{A}}{\partial t}+\sigma\nabla\phi=0 \tag{2.18}$$

An additional equation for the magnetic vector potential and electric scalar potential is obtained from the continuity condition

$$\nabla \cdot \mathbf{J} = 0 \tag{2.19}$$

which is acquired by calculating the divergence of Eq. (2.9). Thus, substituting Eq. (2.16) into Eq. (2.19) results in

$$\nabla \cdot \left(\sigma \frac{\partial \mathbf{A}}{\partial t} \right) + \nabla \cdot \left(\sigma \nabla \phi \right) = 0 \tag{2.20}$$

In the general case, the magnetic field problems involve four unknown quantities: three components of the magnetic vector potential and the electric scalar potential. The unknowns are functions of the three spatial coordinates and time. Solution of three-dimensional fields requires immense computational time and is often impracticable. However, the great majority of the magnetic field problems are solved using a two-dimensional approximation, which is based on the assumption that the magnetic field does not depend on *z*-coordinate (*z*-axis being parallel to the axis of rotor shaft). Thus, the magnetic field is solved in the plane of the machine's cross section (*x*-*y* plane). The current density and magnetic vector potential in two-dimensional problems only have the *z*-components

$$\mathbf{A} = A(x, y, t)\mathbf{e}_z \tag{2.21}$$

$$\mathbf{J} = J(x, y, t)\mathbf{e}_z \tag{2.22}$$

here, $\mathbf{e}_z$ is unit-vector parallel to *z*-axis.

Expressions (2.21) and (2.22) cannot, though, be used for electrical machines with skewed geometries. However, the effects of skewing are beyond the scope of this work.

2.2 Calculation of electromagnetic force

There are several techniques available for computing electromagnetic force. These are based on different formulations and can be classified into two categories (Bastos and Sadowski, 2003):

- methods based on the results directly obtained by solving the magnetic vector potential equation;
- methods based on the force density over the magnetic material surfaces.

In the second category, there are several approaches based on the application of equivalent sources: currents, magnetic charges and combination of magnetic charges and currents. The main idea of these techniques is to replace a magnetic material with a nonmagnetic material having a superficial distribution of currents or magnetic charges or both on its surface. Application of the methods based on the force density requires a bigger computational effort compared to the methods based on "direct formulation". Therefore, the former are not considered in this work.

The first category includes the following methods:

1. the co-energy variation method;
2. the Maxwell stress tensor method;
3. the method proposed by Arkkio;
4. the method of local Jacobian matrix derivation.

The co-energy variation method

This technique, sometimes also referred as the virtual work method, can be employed to calculate the electromagnetic force in electrical machines with constant current (Bastos and Sadowski, 2003). Therefore, it has a limited application area. As implied by the name of this approach, the co-energy of the magnetic field is involved

$$W' = \int_V \left[\int_0^H B \mathrm{d}H \right] \mathrm{d}V \tag{2.23}$$

here, V is integration volume.

The force acting along the direction of virtual displacement of the body can now be calculated as the derivative of the magnetic co-energy of this body with respect to the virtual displacement

$$F_x = \left. \frac{\mathrm{d}W'}{\mathrm{d}x} \right|_{i=\text{constant}} \tag{2.24}$$

here, F_x is force acting along the x-direction.

In order to calculate the co-energy derivative in Eq. (2.24), two magnetic field solutions are required. These must be obtained with a constant current value and with a rotor displaced by a distance dx between the two calculation points. Therefore, this technique becomes tedious for the calculation of the electromagnetic force in electrical machines supplied by the power converters.

The Maxwell stress tensor

The Maxwell stress tensor is one of the most efficient general methods to calculate the forces on bodies placed in the magnetic field. Application of this method requires the body to be located in the air or within a material with permeability $\mu = \mu_0$. Moreover, the magnetic field has to be known on the whole surface enclosing the body. Therefore, this technique is commonly used in conjunction with the numerical computation of the magnetic field.

Application of the Maxwell stress tensor facilitates understanding of the relationships between the magnitudes and directions of the magnetic fields and the forces they generate. The stress tensor expressed in terms of the flux density components is (Luomi, 1993)

$$\tau = \frac{1}{\mu_0}\begin{bmatrix} B_x^2 - \frac{1}{2}B^2 & B_x B_y & B_x B_z \\ B_y B_x & B_y^2 - \frac{1}{2}B^2 & B_y B_z \\ B_z B_x & B_z B_y & B_z^2 - \frac{1}{2}B^2 \end{bmatrix} \tag{2.25}$$

here, B_x, B_y and B_z are components of the magnetic flux density in x-, y- and z-directions, respectively.

The Maxwell stress tensor is defined in such a way that the force density f is obtained as its divergence

$$f = \nabla \cdot \tau \tag{2.26}$$

The total electromagnetic force is calculated by integrating the force density over the region containing the body

$$\mathbf{F} = \int_V f \,\mathrm{d}V \tag{2.27}$$

Substituting Eq. (2.26) into Eq. (2.27) and applying Gauss's theorem yields

$$\mathbf{F} = \int_V f \,\mathrm{d}V = \int_V \nabla \cdot \tau \,\mathrm{d}V = \oint_S \tau \cdot \mathbf{n} \,\mathrm{d}S \tag{2.28}$$

here, $\mathbf{n}$ is unit-vector normal to the boundary S of the region V.

The force is now evaluated as an integral over the boundary S of the region V. When studying radial-flux electrical machines, it is often assumed that the magnetic flux density does not have a z-component. Thus, in the cross section of the machine, the magnetic flux density can be resolved into two orthogonal components: B_n, which is normal to the boundary S and B_t, which is tangential to the boundary S. Thus, the magnetic flux density vector becomes

$$\mathbf{B} = B_n\mathbf{n} + B_t\mathbf{t} \tag{2.29}$$

here, $\mathbf{t}$ is unit-vector tangential to the boundary S.

Expression (2.28) can now be rewritten

$$\mathbf{F} = \oint_S \left(\frac{1}{\mu_0} B_n \mathbf{B} - \frac{1}{2\mu_0} B^2 \mathbf{n} \right) \mathrm{d}S = \oint_S \left(\frac{1}{2\mu_0} \left(B_n^2 - B_t^2 \right) \mathbf{n} + \frac{1}{\mu_0} B_n B_t \mathbf{t} \right) \mathrm{d}S \tag{2.30}$$

For two-dimensional analysis of an electrical machine, Eq. (2.30) can also be written in another form, wherein the surface integral is reduced to the line integral

$$\mathbf{F} = l_\mathrm{e} r \int_0^{2\pi} \left[\frac{1}{2\mu_0} \left(B_n^2 - B_t^2 \right) \mathbf{n} + \frac{1}{\mu_0} B_n B_t \mathbf{t} \right] \mathrm{d}\varphi \tag{2.31}$$

here, r is radius of the integration contour.

In radial-flux electrical machines, it is often assumed that the normal magnetic flux density component is significantly larger than the tangential one and the latter is, therefore, ignored. Thus, Eq. (2.31) can be simplified

$$\mathbf{F} = \frac{l_\mathrm{e} r}{2\mu_0} \int_0^{2\pi} B_n^2 \mathbf{n}\ \mathrm{d}\varphi \tag{2.32}$$

Method proposed by Arkkio

In theory, the solution of Eq. (2.31) should be independent of the choice of the integration-path radius r, as long as the latter is within the confines of the inner (r_r) and outer (r_s) radii of the air gap. In practice, though, the result of Eq. (2.31) can vary substantially as a function of r (Arkkio, 1987). To overcome this problem, Arkkio suggested the computation of the electromagnetic force as the surface integral, limited by the radii r_r and r_s

$$\left(r_\mathrm{s} - r_\mathrm{r} \right) \mathbf{F} = \int_{r_\mathrm{r}}^{r_\mathrm{s}} \mathbf{F} \mathrm{d}r \tag{2.33}$$

Using Eq. (2.31) in Eq. (2.33) and noting that $l_\mathrm{e} r \mathrm{d}\varphi = \mathrm{d}S$ yields

$$\mathbf{F} = \frac{l_e}{(r_s - r_r)} \int_{S_{ag}} \left[\frac{1}{2\mu_0} \left(B_n^2 - B_t^2 \right) \mathbf{n} + \frac{1}{\mu_0} B_n B_t \mathbf{t} \right] \mathrm{d}S \tag{2.34}$$

here, S_{ag} is area of the air gap cross section.

The method of local Jacobian matrix derivation

This technique, developed by Coulomb (1983), is based on the principle of virtual work and is implemented in the FEA. Similarly to the Maxwell stress tensor, this approach applies to a movable body surrounded with free space. The co-energy functional of the domain discretised into the finite elements is computed

$$W_c = \int_V \left(\int_0^H \mathbf{B} \cdot \mathrm{d}\mathbf{H} \right) \mathrm{d}V + \int_S \psi B_r \cdot \mathrm{d}S \tag{2.35}$$

here, ψ is magnetic scalar potential.

The force in x-direction is calculated as the derivative of the functional with respect to the virtual displacement in x-direction

$$F_x = \frac{\mathrm{d}W_c}{\mathrm{d}x} \tag{2.36}$$

Substituting Eq. (2.35) into Eq. (2.36) and using local coordinates instead of the global ones for the subset of virtually distorted finite elements (elements between the movable and fixed parts) yields

$$F_x = \sum_e \int_{V_e} \left[-\mathbf{B}^T \cdot \mathbf{G}^{-1} \cdot \frac{\partial \mathbf{G}}{\partial x} \cdot \mathbf{H} + \int_0^H \mathbf{B} \cdot \mathrm{d}\mathbf{H} \cdot |\mathbf{G}|^{-1} \cdot \frac{\partial |\mathbf{G}|}{\partial x} \right] \mathrm{d}V \tag{2.37}$$

here, $\mathbf{G}$ is the Jacobian matrix ($\mathbf{G} = \left[\frac{\partial}{\partial u}, \frac{\partial}{\partial v}, \frac{\partial}{\partial w} \right]^T [x, y, z]$) coupling the local coordinates to the global ones, $|\mathbf{G}|$ is the determinant of the Jacobian matrix.

In Eq. (2.37), the summation is performed over the air gap elements that can be virtually deformed by the motion of mobile parts.

Accuracy of the numerical methods for electromagnetic force calculation

Each of the FEM-based force computation techniques offers its own advantages. To attain the same accuracy, the classical virtual work method can use a much coarser mesh than the one required for the Maxwell stress method (Mizia et al., 1988). Besides, the accuracy of latter technique depends also on the choice of the integration contour. On the other hand, numerical differentiation of the co-energy can introduce significant errors. Technique developed by Coulomb (1983) can avoid this round-off error of the virtual work method. The method developed by Arkkio eliminates the dependence of the solution on the choice of the integration contour.

As the Maxwell stress tensor is commonly applied for the electromagnetic force calculation in electrical motors, some techniques to improve the accuracy of this finite-element-based method are summarized below:

1. high order finite elements are applied, especially at the interfaces of different magnetic media;
2. it is advisable to decrease the element size, i.e., increase the number of finite elements, especially at the corners of iron parts and in the air gap (Wignall et al., 1988). Particularly, in the regions where the magnetic flux density varies in magnitude and direction a denser finite-element mesh should be applied;
3. a magnetic vector potential formulation of the magnetic field is more suitable for the calculation of the normal component of the magnetic force, while the scalar magnetic potential formulation is more appropriate to compute the tangential force or torque (Cai et al., 2001);
4. in the ascending order of accuracy of the magnetic force calculation, the finite elements can be grouped as: first-order triangular elements, second-order triangular elements, first-order quadrilateral elements, second-order quadrilateral elements (Tarnhuvud and Reichert, 1988). Wignall et al. (1988) recommend to choose as rectangular finite-element shape as possible. A technique to generate the triangular elements from the rectangular ones is discussed in (Sadowski et al., 1992);
5. integration contour should pass through the element's central point as the values at this point are more accurate than at the other points within the finite element (Reichert et al., 1976.);
6. integration contour should lie as far as possible from the iron parts or laminations (Mizia et al., 1988). Moreover, integration contour should not lie on the boundaries dividing the finite element layers in the air gap. The integration contour is best chosen halfway between the stator and rotor surfaces. Thus, using at least three layers of finite element in the air gap is recommended (Cai et al., 2001).

2.3 Literature review

During the history of electrical motors, many different approaches were developed for magnetic field analysis and electromagnetic force calculation in electrical machines with eccentric rotors. These can generally be grouped into two main categories:

- analytical methods;
- numerical methods.

Evolution of each of these approaches is presented in detail below.

2.3.1 Analytical methods

According to DeBortoli et al. (1993), problems related to rotor eccentricity in electrical machines have been discussed for more than a century (Fisher-Hinnen, 1899). Rosenberg (1918) mentioned that imperfect erection or bending of the machine's shaft, or slight subsidence of the foundations with consequent distortion of the bedplate, may cause a displacement of the rotor and stator centres. Even if they are perfectly concentric while the machine is cold, the uneven thermal expansion may cause a distortion of the frame and shifting of the stator centre. To evaluate the UMP in eccentric-rotor machines, Rosenberg used the difference in the magnetic flux densities over the opposite poles. The magnetic flux densities were established from the magnetisation curves of the machine.

Robinson (1943) attempted to analytically describe the UMP due to the static rotor eccentricity in induction and synchronous motors. For induction machines, the UMP was simply expressed as a product of stator bore area and squared magnetic flux density multiplied by a certain factor. To account for sinusoidal flux distribution, tooth-tip saturation and the influence of parallel stator windings the corresponding factors were applied. As for the synchronous motor, the UMP was calculated using the equation developed for an induction machine, where another factor, accounting for the different shape of the magnetic field, was introduced.

It has also been long known that parallel windings effectively mitigate the UMP (Hellmund, 1907). Robinson (1943) and Krondl (1956) tried to analytically model the effects of parallel stator paths on the UMP. Schuisky (1971) stated that the rotating magnetic fields are damped by the rotor cage to varying degrees, depending on their pole number.

Summers (1955) began to develop the theory of UMP based on the rotating magnetic field components. Using the rotating field theory, Robinson (1963) showed mathematically, and also by physical reasoning, that in alternating-current machines with rotating magnetic field in the air gap, the rotor can vibrate at the line frequency and twice the line frequency. Frohne (1967) explained the occurrence of the UMP as a result of the interaction between the magnetic field harmonics with numbers of pole-pairs differing by one.

Theoretical studies of the UMP generated by the fundamental magnetic field component together with magnetic field harmonics having a lower and higher number of poles were presented by Freise and Jordan (1962) and Jordan et al. (1967). The occurrence of the magnetic field harmonics is explained by the modulation of the fundamental MMF wave by the air gap permeance, consisting of a constant component and a series of sinusoidal waves. It was pointed out that, in two-pole motors, a homopolar flux, which crosses the air gap only once and returns through the shaft, bearings and casing, can occur. Therefore, some authors did not consider two-pole machines as these presented a special case (Binns and Dye, 1973). Covo (1954), however, did not make any distinction between the machines having two or more poles. Yet, he concluded that his findings were not valid for two-pole motors.

The homopolar flux and the resultant UMP in two-pole induction motors were further investigated by Haase et al. (1972), Kovacs (1977), Belmans et al. (1982a, 1982b). The relationship between the UMP and homopolar flux generated by a statically eccentric rotor was also considered by Belmans et al. (1987). The authors showed that, due to this kind of eccentricity, a homopolar flux is generated having the supply frequency and yielding a vibrational component of the UMP with two-times the supply frequency.

Yang (1975) employed rotating field theory to investigate the acoustic noise emitted from two-pole single-phase induction motors, primarily due to radial vibrations. He also studied the effects of homopolar flux caused by the static and dynamic eccentricities on the noise and vibration. He showed that the homopolar flux waves play a key role in generating a series of radial force waves having the amplitudes pulsating at twice the slip frequency. The author also pointed out that a number of other low-frequency radial force waves are produced by the homopolar flux. His conclusions are often quoted in the literature and sometimes applied in the analysis of noise and vibration in single-phase machines having more than two poles (Timar, 1989). Zhu and Howe (1997) generalised the theory presented by Yang (1975) to be applicable to the machines having any number of poles and also to account for the effects of magnetic circuit saturation. Based on their experimental results, they stated that the acoustic noise generated by the fan in their motor/fan assembly is not as important as the electromagnetically induced noise. However, the fans do amplify the effect of the rotor unbalance due to its eccentricity, and, hence, serve to increase the electromagnetic noise and vibration emitted by the motor.

A novel analytical approach to studying the UMP was developed by Smith and Dorrell (1996). Their technique was based on the generalised harmonic analysis (Williamson, 1983), which earlier proved successful in studying faults in the stator winding, rotor cage, end- and inter-rings (Williamson and Smith, 1982), (Williamson and Mirzoian, 1985), (Williamson and Abdel-Magied, 1987) and (Williamson and Adams, 1989). The generalised harmonic analysis relies on the calculation of coupling impedances, which relate voltages applied across any winding to the currents flowing in various circuits within the machine. Therefore, this approach could be applied to the analysis of any series/parallel-winding connections. Dorrell and Smith (1994) also used this method, together with the conformal transformation technique (Swann, 1963), to calculate the UMP in induction motors with parallel stator windings. They showed that parallel stator windings shift the direction of the UMP from the direction of rotor eccentricity.

Ellison and Moore (1968) and Heller and Jokl (1969) applied a permeance harmonic analysis to straightforwardly model the magnetic fields in the air gap of an electrical machine. According to Vandevelde and Melkebeek (1994), this technique allows the effortless incorporation of the effects of rotor eccentricity, saturation and slotting into the magnetic field analysis. Based on the permeance harmonic theory, Fruchtenicht et al. (1982) presented an analytical method to investigate the electromagnetic forces in induction machines with rotor whirling at various frequencies. Berman (1993) applied a classical permeance harmonic analysis to study the effects of equalising connections in the stator winding of induction machines with static and dynamic rotor eccentricities. His calculations revealed that the radial magnetic forces can be significantly reduced by means of equalising connections in the stator winding. These findings were also confirmed by the experiments. Stavrou and Penman (2001) also applied the permeance harmonic theory to develop a general model of induction machines with dynamic rotor eccentricity. In order to calculate the MMF, winding distribution was modelled by the so-called winding variable. They proposed to use an effective dynamic eccentricity value in order to account for the circulating currents, saturation, internal current redistribution and flux fringing in open slots.

There also are numerous contributions in which the rotor eccentricity was studied using techniques based on the Winding Function Approach (WFA) presented by Lipo

(1987). WFA is based on the fundamental geometry and winding layout of an arbitrary *n*-phase machine. The stator and rotor circuits are assumed to be independent and can be connected in any fashion to form the stator winding phases and rotor bar/end-ring configuration to be investigated. WFA allows all the space harmonics to be taken into account when calculating the inductances. This method was successfully applied to model the induction machine with arbitrary winding layout and/or unbalanced operating conditions (Luo et al., 1995), (Toliyat and Lipo, 1995), (Milimonfared et at., 1999) and (Nandi and Toliyat, 2002). Joksimovic and Penman (2000) employed WFA to address the rotor bar skewing. The influence of rotor bar skewing and linear MMF rise across the slots on the motor's inductances was investigated by Joksimovic et al. (1999). However, in its original formulation, the WFA could only be applied to those machines where there existed a symmetry in the radial air gap and where the air gap was uniform, i.e. motors without the rotor eccentricity (Al-Nuaim and Toliyat, 1997). To overcome this problem, a Modified Winding Function Approach (MWFA) was developed (Toliyat and Al-Nuaim, 1997). In the MWFA, the difference of MMF drop in the air gap on both sides of the eccentric rotor was taken into account when computing the inductances. This technique was applied to model a salient-pole synchronous machine with dynamic rotor eccentricity (Al-Nuaim and Toliyat, 1998) and an induction machine with static, dynamic and mixed eccentricities (Nandi et al., 1997), (Nandi et al., 1998), (Nandi et al., 2001). Rotor skewing and linear rise of the MMF over the slot in an induction machine with dynamic eccentricity were studied by Joksimovic et al. (2000). Another method of addressing the axial non-uniformity due to the rotor skewing in induction machines with static and dynamic eccentricity was presented by Bossio et al. (2004). All these techniques were based on the WFA. However, the radial forces due to the rotor eccentricity were not studied using WFA-based techniques. It has mainly been applied to calculate the inductances and currents of electrical machines.

The static and dynamic rotor eccentricities in a switched reluctance motor were investigated by Garrigan et al. (1999). They developed a magnetic equivalent circuit approach that allowed accurate and quick force prediction. The authors showed that, in a switched reluctance machine, the unbalanced force grows almost linearly with the increasing relative rotor eccentricity (up to 20-25% of the nominal air gap). At a larger rotor axis displacement from its centred position, the rate of the force increase drops off. This UMP reduction was associated with the onset of saturation in the region where the air gap is reduced. The authors also mentioned that the eccentric rotor may whirl forwards, backwards, synchronously, sub- and super-synchronously. The parallel connected windings were found to naturally and significantly reduce (by a factor of three or even four) the UMP.

Kim and Lieu (1998) developed an analytical technique to calculate the instantaneous magnetic field distribution in the air gap of a permanent magnet motor with rotor eccentricity. Li et al. (2007) applied a conformal transformation technique (Swann, 1963) to analytically calculate the magnetic field in the air gap of a permanent magnet motor. Applying the rotating field theory, Dorrell et al. (2003) presented a mathematical model to compute the radial force on the eccentric rotor of an interior permanent magnet motor equipped with the levitation and main windings. The results of these analytical methods compared well with numerical simulation results.

Dorrell (1995a, 1996) examined the effects of rotor cage skewing on the UMP magnitude. He showed that skewing increases the UMP in a loaded machine, but has little effect at no load. These findings compared well to the measurements.

A study on the UMP reduction due to iron saturation in eccentric-rotor induction machines was presented by Dorrell (1999). He also reviewed and explained in simple terms other circumstances affecting the UMP magnitude, such as parallel connections in the stator and rotor windings and transient and variable-frequency operation of the machine.

Using rotational field theory, Dorrell (2000) presented an analytical method to investigate the non-uniform rotor eccentricities, i.e. the eccentricities with the rotor and stator axes not being parallel to each other.

Electromagnetic forces in eccentric-rotor motors were also considered from the mechanical point of view. Kovacs (1977) mentioned that UMP behaves as a spring force with a negative spring constant. Fruchtenicht et al. (1982) showed that, due to the currents in the rotor cage, a tangential UMP component is produced. This component, which has often been neglected in the past, behaves as a damping force and can assume both positive and negative values. Belmans et al. (1985) showed that UMP due to the rotor eccentricity has to be taken into consideration when analysing the electromechanical vibrational behaviour of the flexible-shaft machine. They also used a negative electromagnetically induced spring constant and introduced a negative electromagnetically induced damping coefficient. It was pointed out that a negative spring constant lowers the critical speed of the machine. The negative electromagnetically induced damping coefficient has to be subtracted from the positive mechanical damping coefficient; this might yield unstable rotor vibrations if the value of the former exceeds the value of the latter.

As long ago as 1918, a review of the bibliography on the subject of UMP in electrical machines was published by Gray and Pertsch (1918). More recent literature surveys related to this topic were presented by von Kaehne (1963) and Binns and Dye (1973). The latest work is reviewed by Dorrell (1993) and Tenhunen (2003). A fresh literature survey from the perspective of electromechanical interaction in electrical machines has been written by Holopainen (2004).

2.3.2 Numerical methods

Finite Element Method (FEM) is a general numerical technique, which is used for finding an approximate solution of partial differential equations as well as of integral equations. FEM finds applications in various engineering areas, such as structural analysis, fluid dynamics, electromagnetism, thermal analysis, etc. Other common numerical methods are: Boundary Element Methods, Finite Difference Methods, Finite Volume Methods, and Spectral methods. Meshless (also called "meshfree") methods are a recently developed class of numerical methods. However, FEM remains the dominating method in engineering analysis for several reasons:

- FEM formulation handles complex geometry and varying boundary conditions well;
- it is easy to develop a general code, handling several problem types;
- there exists a large amount of tested and efficient codes with easy to use interfaces.

According to Felippa (2001), the best summary of the early history of FEM from circa 1800 B.C. through 1970, is given in Chapter 1 of the textbook by Martin and Carey (1973). The basic principles of FEM and its application for the analysis of electromagnetic fields in electrical machines are given by Chari and Silvester (1980), Arkkio (1987), Silvester and Ferrari (1996) and Luomi (1993). A three-dimensional FEA of the electromagnetic field is presented in (Chari et al., 1982).

The wide spread use of the numerical calculation techniques is closely related to the evolution of digital computers. However, even with such powerful computers as are available today, the FEA of three-dimensional, time-dependent problems involving complex geometries (such as those of electrical machines, for example) is quite a time consuming task. It is, therefore, a common practice to solve the magnetic field in two dimensions, assuming it to be independent of the coordinate parallel to the machine's shaft. In this case, the three-dimensional effects such as the rotor-cage skewing and end-windings fields must be separately accounted for in the two-dimensional formulation (Arkkio, 1987).

Using a two-dimensional magnetic field formulation, Arkkio and Lindgren (1994) calculated the electromagnetic forces acting on an eccentric rotor of a high-speed induction machine. The magnetic field and electrical circuit equations for the windings were solved together as a system of equations. The forces were calculated from the air-gap field using a method based on the principle of virtual work. The calculation was accomplished by the time-stepping FEA. Research has revealed that non-symmetric flux distribution caused by eccentricity induces eddy currents in the rotor conductors. These currents reduce the UMP significantly. It was noticed that the increasing supply voltage frequency decreases the magnitude of the total electromagnetic force and changes its direction. Later on, Arkkio (1996) extended the numerical analysis of the electromagnetic forces due to the static and dynamic rotor eccentricities to the conventional cage induction motors. The effects of parallel branches in the stator winding, iron saturation and loading of the machine were given more attention. As a result, it was shown that the iron bridges of closed rotor slots provide a path for the non-symmetric flux, along which it can flow without generating equalising currents in the rotor cage. Thus, at no load, a motor with closed rotor slots may produce a larger unbalanced pull than the motor with semi-open slots. A FEA-based study of the UMP due to the broken rotor bar(s), end-ring, improper number of rotor slots and static and dynamic rotor eccentricities in cage induction motors is reported in (Arkkio, 1997). The influence of parallel stator windings, iron saturation and motor loading on the UMP was also investigated. It was shown that the eccentricity forces increase with the load. Dorrell (1995b) found that this phenomenon is caused by the higher magnetic field harmonics in the air gap.

Extensive numerical studies on the UMP reduction by various combinations of parallel stator windings in an induction machine were undertaken by Salon et al. (1992) and DeBortoli et al. (1993). They considered both static and dynamic rotor eccentricities and showed that currents circulating between the parallel stator windings lessen the UMP considerably. Moreover, the researchers observed that the circulating currents also diminish or eliminate other vibration-producing magnetic force harmonics generated by the rotor eccentricity.

Numerical analysis into the vibrational behaviour of the switched reluctance motor is given in (Neves et al., 1998). Forces acting upon the stator were evaluated using the local force density method. The authors concluded that a two-dimensional model is sufficient for analysing mechanical vibrations created by electromagnetic phenomena in a switched reluctance motor.

Salon et al. (2001) studied the influence of rotor eccentricity on the torque ripple in a surface mounted brushless DC motor. Using the numerical simulation, authors observed that the torque ripples were virtually unaffected by small eccentricities (relative rotor eccentricity up to 30% were studied). In surface mounted permanent magnet motors, the magnets significantly increase the effective air gap. Therefore, small changes in the actual air gap due to the rotor eccentricity translate to negligible changes in the effective air gap of the motor. As a result, the surface mounted permanent magnet motors are less susceptible to the air gap asymmetry compared to induction motors.

Using FEA, Kyung-Tae Kim et al. (2001) studied the magnetic field and the electromagnetic force in interior- and surface mounted permanent magnet motors with rotor eccentricity. Authors concluded that in the interior permanent magnet motor, rotor eccentricity causes a substantially stronger magnetic field asymmetry and unbalanced magnetic force, compared to the surface mounted permanent magnet motor.

Using the FEA, Lundstrom et al. (2007) have calculated the electromagnetic force caused by the rotor eccentricity in a large synchronous hydrogenerator. Authors reported that the damper winding substantially reduced the unbalanced electromagnetic force and also introduced a force component perpendicular to the eccentricity axis. The stability and eigenfrequencies of the rotor were also shown to be affected by the damper winding.

Applying FEM-based simulations, Perers et al. (2007) showed that iron saturation has a significant impact on the magnetic field harmonics and UMP in a large salient-pole synchronous machine with static rotor eccentricity. As the saturation increases, when the machine is loaded, the eccentricity harmonics and the unbalanced electromagnetic force are reduced.

Lantto et al. (2000) investigated the induction motor with eccentric rotor whirling at different whirling frequencies. They validated the finite element model of the motor by measurements.

Schlensok and Henneberger (2004) built FEM models of an induction machine with concentric and eccentric rotors to calculate the torque, total force acting on the rotor and surface force density on the stator teeth. The results showed that dynamic rotor eccentricity has a minor effect on the average torque of the machine: the average torque magnitude was slightly reduced due to the rotor eccentricity. However, the eccentricity exhibited a strong impact on the surface force density distribution on the stator inner surface.

Cylindrical and conical rotor eccentricities were investigated by Tenhunen (2001), who developed a so-called multi-slice FEM model of an induction machine. He used a two-dimensional field formulation, however, to account for the axial variation in the geometry of the motor. The magnetic field was calculated on a set of cross sections of the motor perpendicular to the stator shaft. The UMP and equalising currents in the parallel stator windings were computed for static and dynamic eccentricities.

Using the FEA, Tenhunen et al. (2003a) studied the UMP in an induction machine as a function of whirling frequency. They developed a numerical impulse response test to calculate the frequency response of the electromagnetic forces, from which the UMP in a wide whirling frequency range could readily be established. The impulse response test was realised in the numerical simulation by moving the rotor from its centred position for a short period of time and recording the excitation and response signals of the system. From these, the frequency response of the electromagnetic force was calculated by applying spectral analysis techniques. The forces calculated by this method were compared with those from the conventional FEA technique (forced whirling method) and showed a very good agreement. Using the impulse test, the UMP in a required whirling frequency range was calculated from the results of a single FEM simulation, thus providing up to 95% savings in the computation time. The accuracy of the method also seemed to be very good.

After its introduction, the numerical impulse response test was applied to study the effects of equalizing currents in the rotor cage and parallel stator windings on the UMP in eccentric-rotor induction motor (Tenhunen et al., 2003b). Using this technique, Tenhunen et al. (2003c, 2003d) analysed the cylindrical circular whirling motion, symmetric conical whirling motion and the combination of these two basic eccentricity modes, whereas Tenhunen (2005) calculated the eccentricity harmonics of the magnetic flux density in the air gap of an induction motor. Tenhunen et al. (2004) applied the numerical impulse response test to investigate the effects of magnetic saturation on the UMP in induction machines with cylindrical circular rotor eccentricity.

To validate the finite-element models, the numerically computed electromagnetic forces were compared with the measured ones. Tenhunen et al. (2003d) showed that FEA calculation results agreed very well with the measurements. In his study, he considered a standard 15 kW induction motor with different types of rotor eccentricities. Arkkio et al. (2000) and Lantto et al. (2000) reported a very good agreement between the computed and measured electromagnetic forces in a 15 kW induction motor with cylindrical circular rotor eccentricity.

2.3.3 Combining the analytical and numerical methods

Both analytical and numerical methods have their own benefits and drawbacks in studying electrical machines. The beauty of analytical approaches lies in their capability to provide the results promptly and in a form that is simple to interpret. However, problems arise when the effects of magnetic saturation, circulating currents, stator and rotor slotting need to be evaluated accurately. Numerical techniques, on the other hand, offer a high degree of accuracy in the final solution and provide convenient means to address the saturation and other non-linear complicated phenomena encountered in electrical motors. However, they place substantial requirements on the computational power of computers and are time consuming. Moreover, when the phenomenon involved is not transparent, the output of FEM computation is not always lucid and understandable. By combining analytical and numerical techniques, it is possible to build on their strengths and break through their limitations.

Arkkio et al. (2000) investigated numerically the UMP in a standard cage induction motor. The operation of the motor was studied in a wide whirling frequency range using so-called harmonics excitation of the rotor, i.e. the eccentric rotor was forced to whirl around the stator bore axis at a certain whirling frequency. Besides, the rotor also rotated around its own axis. The authors named this technique ‘forced whirling method’. Based on the numerical simulation results and theoretical analysis of induction motor presented in (Fruchtenicht et al., 1982), the authors concluded that a relationship between the UMP and eccentric motion of the rotor can be expressed in a simple parametric form

$$\underline{F}_{\mathrm{e}}\left(\mathrm{j}\omega_{\mathrm{ecc}}\right)=\underline{K}\left(\mathrm{j}\omega_{\mathrm{ecc}}\right)\underline{\delta}_{\mathrm{ecc}}\left(\mathrm{j}\omega_{\mathrm{ecc}}\right) \tag{2.38}$$

here, $\underline{F}_{\mathrm{e}}$ is UMP, $\underline{K}$ is Frequency Response Function (FRF) of the UMP, $\underline{\delta}_{\mathrm{ecc}}$ is rotor eccentricity, ω_{ecc} is whirling angular speed.

The FRF is

$$\underline{K}\left(\mathrm{j}\omega_{\mathrm{ecc}}\right)=k_0+\frac{k_{p-1}}{\mathrm{j}\omega_{\mathrm{ecc}}-\underline{z}_{p-1}}+\frac{k_{p+1}}{\mathrm{j}\omega_{\mathrm{ecc}}-\underline{z}_{p+1}} \tag{2.39}$$

here, k parameters are real-valued variables proportional to the square of fundamental magnetic flux density; z parameters are complex-valued variables, whose imaginary parts are defined by the supply and whirling motion frequencies.

The unknown parameters were estimated from the numerical calculation of the machine. Thus, the effects of magnetic saturation, stator and rotor slotting and equalising currents flowing in the rotor cage were addressed in the UMP model (Eq. (2.38)). UMP obtained from the numerical simulation results was fitted into this model, demonstrating a very good agreement. The calculation results agreed also very well with measurements.

The work was continued by Holopainen et al. (2005a), who studied a transient operation of a cage induction motor with rotor eccentricity of arbitrary trajectory and various whirling frequencies. Using the classical permeance harmonic theory, they presented a parametric UMP model, which was then simplified for the constant flux steady-state operation and cylindrical rotor eccentricity. Unlike the earlier model, the parameters in this model had a physical background, i.e. they were directly related to electrical properties and the geometry of the machine. A more efficient procedure to estimate the model parameters from the numerical calculation results was presented by Holopainen et al. (2005b). This technique was based on implementing the impulse excitation instead of traditional harmonic excitation of the rotor during the time-stepping FEM simulation.

2.4 Need for further research

According to the literature survey presented above, the researchers concentrated their efforts on the induction machines and investigated mainly two special cases of the cylindrical circular rotor whirling: the static and dynamic eccentricity. It is well known that the rotor cage (damper winding) and parallel stator windings reduce the UMP. However, the influence of parallel stator windings on the UMP needs to be investigated further, not only at two special whirling frequency values, but rather in a wide whirling frequency range. It would also be interesting to compare how the UMP is affected by the parallel paths in the rotor and by the parallel paths in the stator. A combined influence of the rotor cage (damper winding) and parallel stator windings has to be investigated deeper as well.

The parametric force models presented by Arkkio et al. (2000) and Holopainen et al. (2005a) allow the convenient assessment of the UMP in a wide whirling frequency range. These models, however, were developed for cage induction motors operated without the parallel stator windings. Thus, their application is quite limited, since many electrical machines do contain parallel paths in the stator winding. Therefore, there is a need for parametric force models, which could be applied to electrical machines equipped with parallel stator windings. Besides, a cage induction motor represents only one common type of electrical machine. A salient-pole synchronous machine, which belongs to another major category of electrical machines, should also be taken into consideration. Moreover, special force models are needed for electrical machines with parallel paths both in the rotor and stator windings.

2.5 Conclusions

The basic laws of electromagnetism describing the interrelationships between the electric field, magnetic field, electric current and electric charge are surveyed in this chapter. Different approaches applied for magnetic field analysis and electromagnetic force calculation in rotating electrical machines are briefly reviewed. The origins of the UMP are indicated and the evolution of various analytical and numerical techniques for the analysis of electrical motors operated with rotor eccentricity is also surveyed. An approach combining the strengths of the theoretical and FEM-based methods is described at the end of the chapter. This novel technique allows for accurate, yet quick, calculation of the electromagnetic force in a wide whirling frequency range. It also enables several analyses to be combined effectively in order to investigate simultaneously the electrical machine from electromagnetic, mechanical and thermal points of view.

The parametric models developed so far are only applicable to cage induction motors without the parallel stator windings. The latter not only significantly reduce the UMP magnitude, but also notably alter its whirling frequency dependence. Moreover, the currents circulating in the parallel circuits of the stator may interact with those circulating in the rotor cage, thus introducing additional phenomena that cannot be described by the existing models.

In this thesis, the influence of parallel stator windings on the UMP is investigated numerically. Simple parametric force models are developed for an induction machine and also for a salient-pole synchronous machine equipped with parallel paths in the stator windings. A special UMP model is derived for the motors with parallel circuits both in the rotor and stator windings. The performance of the force models is evaluated based on the comparison with numerical simulation results. This work is also aimed at investigating the interaction between the currents circulating in the parallel paths of the rotor and stator windings.

3 Methods of analysis

As mentioned in the previous chapter, the parallel stator windings considerably reduce the UMP magnitude and also have a potent impact on its whirling frequency dependence. This is shown in Figure 3.1, where the FRFs of the electromagnetic force are calculated numerically for a standard cage induction motor operated at the rated load. The continuous curves represent the radial (upper curve) and tangential (lower curve) components of the UMP when the stator winding is connected in series. The dashed curves show the correspondent UMP components when four parallel paths (4PP) are provided in the stator winding. Corresponding simulation results for a salient-pole synchronous generator operated at the rated load are displayed in Figure 3.2. The main parameters of the simulated machines are listed in Tables 3.1 and 3.2. More data on both the simulated machines can be found in Publication P3.

Table 3.1 Main parameters of the induction motor.

Parameter	Value
Number of pole-pairs	2
Rated frequency, Hz	50
Rated voltage, V	380
Rated power, kW	15
Connection	Delta

Table 3.2 Main parameters of the synchronous machine.

Parameter	Value
Number of pole-pairs	4
Frequency of the voltage supplied to the stator winding, Hz	50
Stator winding supply voltage, V	6300
Field winding supply voltage, V	150
Apparent power, kVA	8400
Stator winding connection	Star

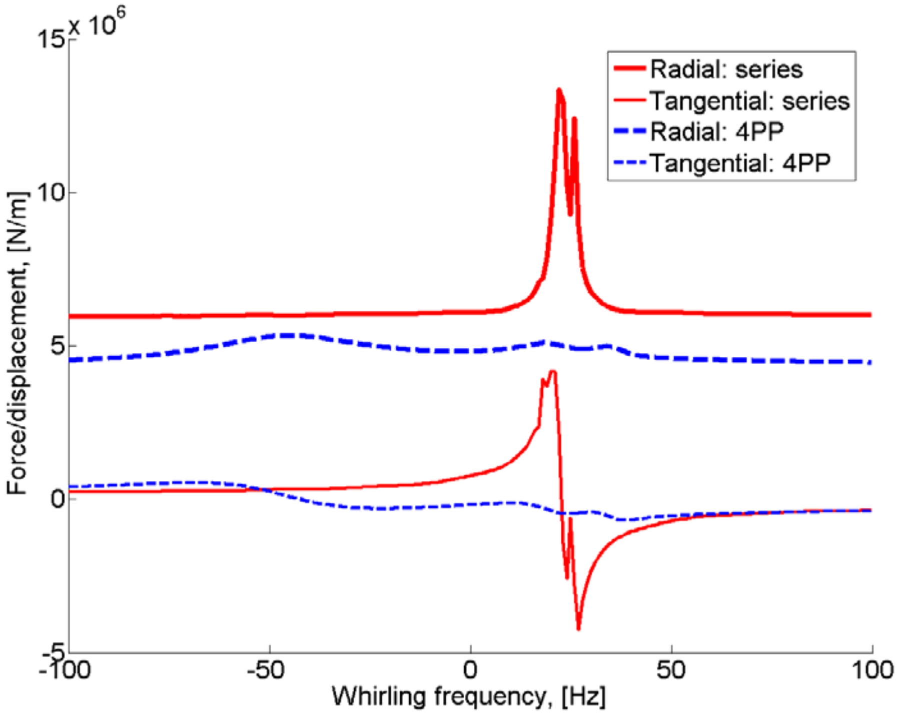

Figure 3.1 Influence of parallel stator windings on the UMP: four-pole, 50 Hz induction motor at the rated load.

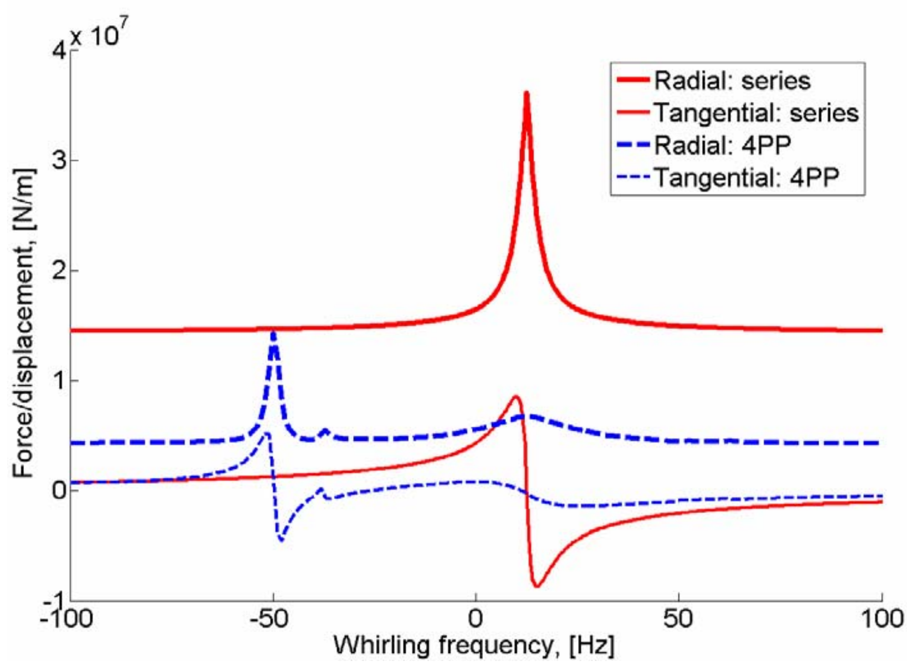

Figure 3.2 Influence of parallel stator windings on the UMP: eight-pole, 50 Hz salient-pole synchronous generator at the rated load.

As seen in Figures 3.1 and 3.2, the two FRFs differ significantly from each other. The parametric force models presented earlier in (Arkkio et al., 2000) and (Holopainen et al., 2005a) are only meant for the induction motors with series-connected stator windings. However, numerous electrical machines do have parallel connections in the stator. Moreover, salient-pole synchronous machines were also beyond the scope of the previous research. In publications P2, P3 and P5, simple UMP models are developed for a salient-pole synchronous machine. The effect of parallel stator windings are included into the force model presented in publication P3. Publication P5 puts forward a parametric force model for electrical machines with parallel windings both in the rotor and stator.

3.1 Parametric force model

The developed force models were derived starting from the basic voltage and magnetic flux equations for the rotor and stator windings. Using the classical permeance harmonic analysis, the influence of rotor eccentricity was introduced through additional magnetic flux density harmonics in the air gap. These harmonics were expressed as functions of fundamental magnetic field, whirling radius, whirling angular speed and corresponding current harmonics flowing in the rotor and/or stator windings. The latter were then solved by substituting the expressions of magnetic flux harmonics into the voltage equations for the corresponding windings and harmonics. Finally, the expression for UMP was derived using Eq. (2.32). In the stationary frame of reference, the parametric model of the UMP in a salient-pole synchronous machine with parallel stator windings and the damper winding is

$$
\begin{aligned}
\underline{K}(\mathrm{j}\omega_{\mathrm{ecc}}) &= \frac{\underline{F}_{\mathrm{e}}}{\delta_{\mathrm{ecc}}\mathrm{e}^{\mathrm{j}(\omega_{\mathrm{ecc}}t-\varphi_{\mathrm{ecc.0}})}} = \frac{\pi d_{\mathrm{r}} l_{\mathrm{e}}}{4\mu_0\delta_0} B_{p,1}\Bigg[\Big(B_{p,1}+B_{p,2}\cos\left(2\varphi_p\right)\Big)+ \\
&\frac{B_{p,1}+B_{p,2}\mathrm{e}^{\mathrm{j}2\varphi_p}}{2A_{p-1}}\Bigg(\left(s\omega_1-\omega_{\mathrm{ecc}}^{\mathrm{r}}\right)\frac{\Big(\left(\omega_1-\omega_{\mathrm{ecc}}\right)\left(L_{\mathrm{s},p-1}-k_{\mathrm{cs},p-1}k_{\mathrm{L,s},p-1}\right)+\mathrm{j}R_{\mathrm{s},p-1}\Big)k_{\mathrm{cr},p-1}k_{\mathrm{L,r},p-1}}{\Big(\underline{S}_{\mathrm{r},p-1,1}+\mathrm{j}\left(s\omega_1-\omega_{\mathrm{ecc}}^{\mathrm{r}}\right)\Big)\Big(\underline{S}_{\mathrm{r},p-1,2}+\mathrm{j}\left(s\omega_1-\omega_{\mathrm{ecc}}^{\mathrm{r}}\right)\Big)}+ \\
&\quad\left(\omega_1-\omega_{\mathrm{ecc}}\right)\frac{\Big(\left(s\omega_1-\omega_{\mathrm{ecc}}^{\mathrm{r}}\right)\left(L_{\mathrm{r},p-1}-k_{\mathrm{cr},p-1}k_{\mathrm{L,r},p-1}\right)+\mathrm{j}R_{\mathrm{r},p-1}\Big)k_{\mathrm{cs},p-1}k_{\mathrm{L,s},p-1}}{\Big(\underline{S}_{\mathrm{s},p-1,1}+\mathrm{j}\left(\omega_1-\omega_{\mathrm{ecc}}\right)\Big)\Big(\underline{S}_{\mathrm{s},p-1,2}+\mathrm{j}\left(\omega_1-\omega_{\mathrm{ecc}}\right)\Big)}\Bigg)+ \\
&\frac{B_{p,1}+B_{p,2}\mathrm{e}^{-\mathrm{j}2\varphi_p}}{2A_{p+1}}\Bigg(\left(s\omega_1+\omega_{\mathrm{ecc}}^{\mathrm{r}}\right)\frac{\Big(\left(\omega_1+\omega_{\mathrm{ecc}}\right)\left(L_{\mathrm{s},p+1}-k_{\mathrm{cs},p+1}k_{\mathrm{L,s},p+1}\right)-\mathrm{j}R_{\mathrm{s},p+1}\Big)k_{\mathrm{cr},p+1}k_{\mathrm{L,r},p+1}}{\Big(\underline{S}^*_{\mathrm{r},p+1,1}-\mathrm{j}\left(s\omega_1+\omega_{\mathrm{ecc}}^{\mathrm{r}}\right)\Big)\Big(\underline{S}^*_{\mathrm{r},p+1,2}-\mathrm{j}\left(s\omega_1+\omega_{\mathrm{ecc}}^{\mathrm{r}}\right)\Big)}+ \\
&\quad\left(\omega_1+\omega_{\mathrm{ecc}}\right)\frac{\Big(\left(s\omega_1+\omega_{\mathrm{ecc}}^{\mathrm{r}}\right)\left(L_{\mathrm{r},p+1}-k_{\mathrm{cr},p+1}k_{\mathrm{L,r},p+1}\right)-\mathrm{j}R_{\mathrm{r},p+1}\Big)k_{\mathrm{cs},p+1}k_{\mathrm{L,s},p+1}}{\Big(\underline{S}^*_{\mathrm{s},p+1,1}-\mathrm{j}\left(\omega_1+\omega_{\mathrm{ecc}}\right)\Big)\Big(\underline{S}^*_{\mathrm{s},p+1,2}-\mathrm{j}\left(\omega_1+\omega_{\mathrm{ecc}}\right)\Big)}\Bigg)\Bigg]
\end{aligned}
\tag{3.1}
$$

here, $\varphi_{\text{ecc.0}}$ is initial phase angle of the rotor eccentricity; δ_0 is nominal air gap; $B_{p,1}$ is the first constituent of the fundamental magnetic flux density component caused by interaction of the fundamental MMF waves with constant permeance term; $B_{p,2}$ is the second constituent of the fundamental magnetic flux density component caused by interaction of the fundamental MMF waves with the first Fourier series component of the air gap permeance related to rotor saliency; φ_p is phase angle between the fundamental magnetic flux density component and the fundamental MMF vector of the field winding; s is slip of the rotor; ω_1 is angular frequency of the supply voltage; $\omega_{\text{ecc}}^{\text{r}}$ is whirling angular velocity in rotor frame of reference; $k_{\text{cr},\,p\pm1}$ are dimensionless coupling factors for $p\pm1$ current harmonics in the damper winding; $k_{\text{cs},\,p\pm1}$ are dimensionless coupling factors for $p\pm1$ current harmonics in the stator winding; $k_{\text{L,r},\,p\pm1}$ are coefficients defining the amounts of the corresponding magnetic flux harmonics that pass through the damper winding from sources other than rotor currents; $k_{\text{L,s},\,p\pm1}$ are coefficients defining the amounts of the corresponding magnetic flux harmonics that pass through the stator winding from sources other than stator currents; $L_{\text{r},\,p\pm1}$ are inductances of the damper winding for $p\pm1$ magnetic flux density harmonics; $L_{\text{s},\,p\pm1}$ are inductances of the stator winding for $p\pm1$ magnetic flux density harmonics; $R_{\text{r},\,p\pm1}$ are resistances of the damper winding for $p\pm1$ current harmonics; $R_{\text{s},\,p\pm1}$ are resistances of the stator winding for $p\pm1$ current harmonics; $A_{p\pm1}$, $\underline{S}_{\text{r},\,p\pm1,1}$, $\underline{S}_{\text{r},\,p\pm1,2}$, $\underline{S}_{\text{s},\,p\pm1,1}$ and $\underline{S}_{\text{s},\,p\pm1,2}$ are force model parameters, which can be expressed in terms of the physical machine parameters listed above.

A synchronous machine in steady state operates with zero slip. However, in expression (3.1), the slip symbol was kept in order to apply this force model to the induction motor as well. To do so, the second constituent of the fundamental magnetic flux density $B_{p,2}$ has to be equated to zero, as this term is related to the rotor saliency. Thus, the force model expression for induction machines becomes a little simpler than Eq. (3.1).

The detailed derivation of the force model (Eq. (3.1)) is given in Publication P5. As can be seen, there are many unknown parameters in the force model expression. Estimation of parameter values is a non-trivial task, which is briefly discussed in the following sub-chapter.

3.2 Parameter estimation

FEM-based simulations of electrical machines provide sufficient data for the estimation of unknown force model parameters. However, as several parameters are encountered in the denominators, a direct application of the least-square method is not possible. For this reason, a hybrid parameter estimation technique was elaborated (Publication P1), which effectively combined the method of least squares with the GA-based approach. The estimation task was shared between the two methods so that the parameters located in the numerators were estimated using the least-square technique, whereas the remaining parameters were estimated using GA. This approach showed superior performance in comparison to the technique where the least-square method was accompanied by the so-called sequential exhaustive search scheme. The supremacy was especially evident when the number of unknown parameters in the denominators was increased. An estimation procedure solely based on the GA was also implemented, demonstrating fairly good performance. However, it required a longer computation time.

3.3 Conclusions

In this chapter, a parametric force model for electrical machines with parallel stator windings and rotor cage (damper winding) is presented. The model is applicable to salient-pole synchronous machines as well as to induction machines. It can also be used for other electrical machines, which feature the parallel paths either in the rotor or stator winding. The technique developed for the estimation of force model parameters is briefly discussed.

4 Discussion of the results

In this chapter, the performance of the parametric force models developed is presented and discussed. Some phenomena arising from the interactions of the currents circulating in the parallel circuits of the rotor and stator are highlighted. The influence of the parallel stator windings on the net UMP and its components is examined. The effects of parallel circuits in the rotor and those in the stator on the eccentricity force are compared. The chapter is based on the data documented in Publications P2-P7.

4.1 Verification of the force models

As mentioned earlier, force models were developed for:

- salient-pole synchronous machines without the parallel stator windings (Publication P2);
- induction and synchronous motors with parallel stator windings, but without the rotor cage (damper winding) (Publication P3);
- induction and synchronous motors with parallel circuits both in the stator and rotor windings (Publication P5).

The first two parametric force models with parameters estimated from the numerical calculation results showed excellent performance. Figure 4.1 demonstrates a very good agreement between the FRF calculated using the FEA and the FRF obtained by substituting the estimated parameters into the force model. These FRFs of the force were computed for the synchronous machine with damper winding only. The performance of the force model applied to synchronous machine with four parallel paths in the stator winding is shown in Figure 4.2. Similar results for the 15 kW cage induction motor with four parallel stator windings are presented in Figure 4.3. In this motor, the influence of the rotor cage on the UMP was annulled in the numerical simulation by using “air” as the material of the rotor cage.

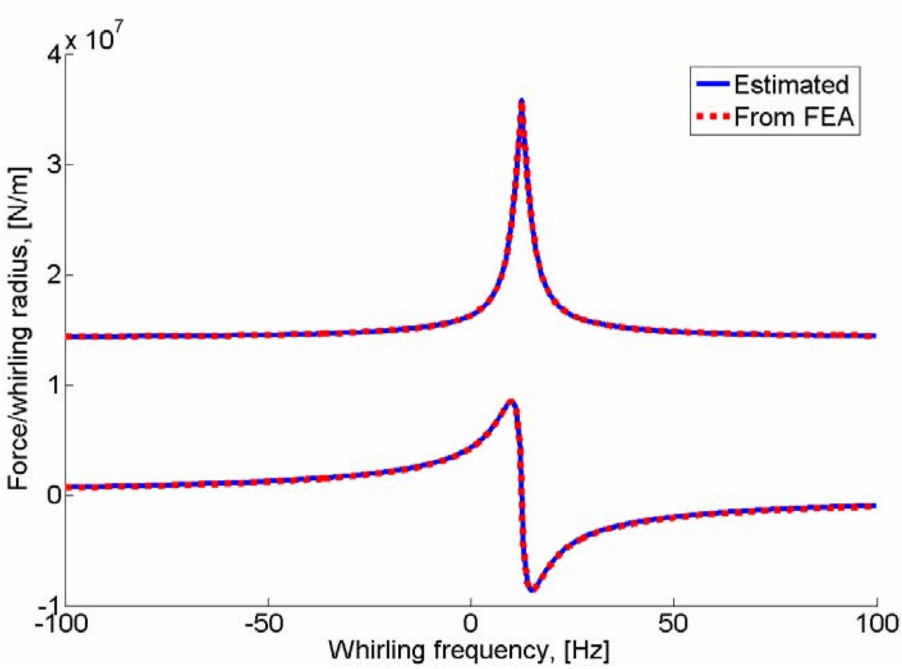

Figure 4.1 FRF calculated numerically vs. FRF obtained using the parametric force model: eight-pole, 50 Hz salient-pole synchronous generator with damper winding and series-connected stator winding at the rated load.

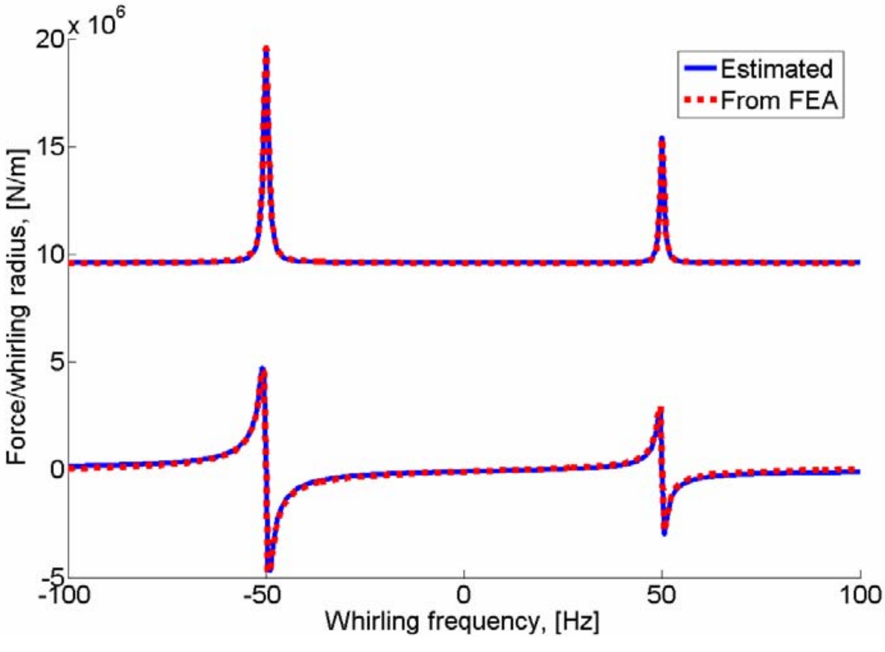

Figure 4.2 FRF calculated numerically vs. FRF obtained using the parametric force model: eight-pole, 50 Hz salient-pole synchronous generator with parallel stator windings but without damper winding at the rated load.

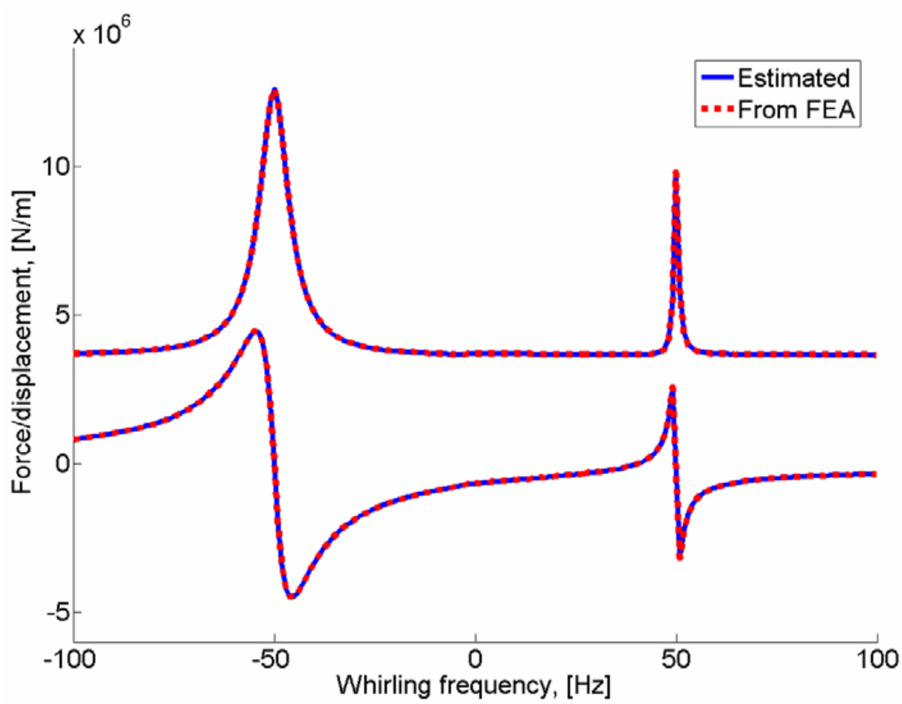

Figure 4.3 FRF calculated numerically vs. FRF obtained using the parametric force model: four-pole, 50 Hz induction motor with parallel stator windings but without rotor cage at no load.

The performance of the force model developed for electrical machines with parallel circuits both in the rotor and stator windings was somewhat worse compared to the two models discussed above; however, it still was very good. In Figures 4.4 and 4.5, FRFs computed using the FEA and parametric force model are compared to each other. The results for the synchronous machine are shown in Figure 4.4 and those for the induction machine – in Figure 4.5. Both the test motors had four parallel stator windings and were operated at the rated load.

As seen in Figure 4.4, there is a small peak in the FRF of the force at whirling frequency –37.5 Hz, which is not accounted for in the force model. The phenomena behind this peak are not clear yet. However, the interaction between the currents circulating in the parallel circuits of the rotor and stator could provide a possible explanation.

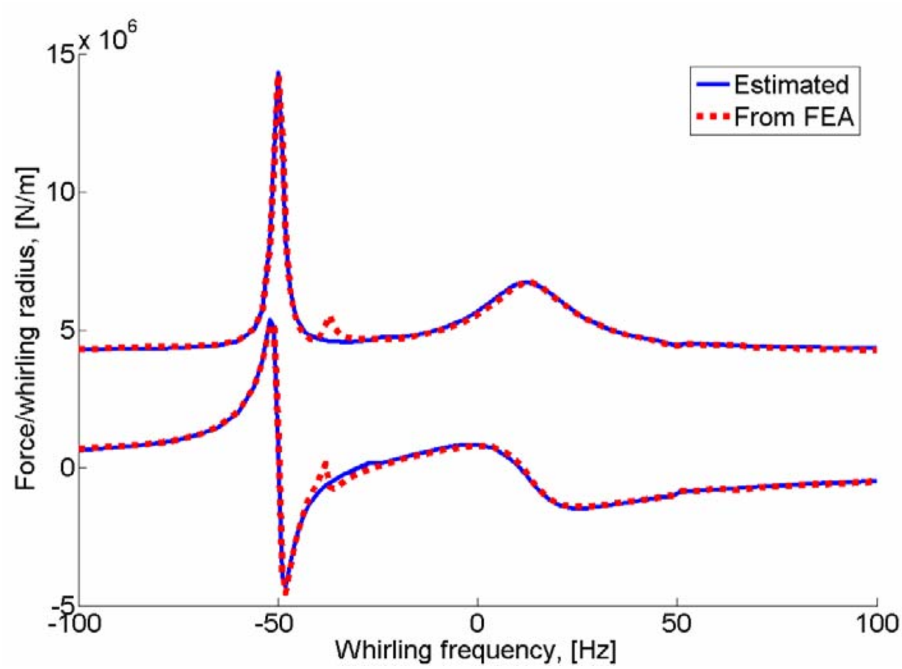

Figure 4.4 FRF calculated numerically vs. FRF obtained using the parametric force model: eight-pole, 50 Hz salient-pole synchronous generator with four parallel stator windings and damper winding at the rated load.

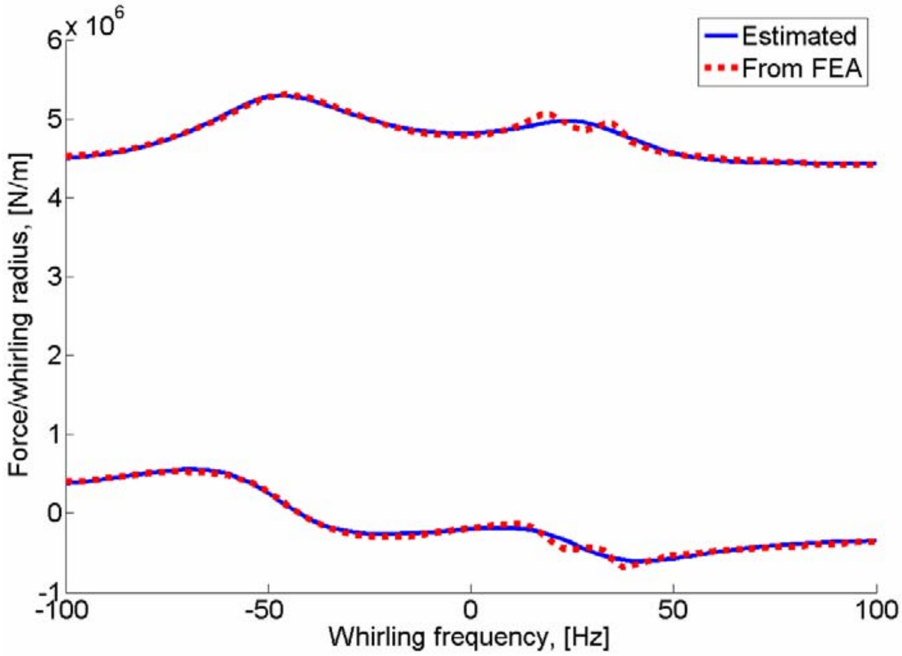

Figure 4.5 FRF calculated numerically vs. FRF obtained using the parametric force model: four-pole, 50 Hz induction motor with four parallel stator windings and rotor cage at the rated load.

The force model developed for electrical machines with parallel circuits both in the rotor and stator windings was also applied to the motors that were equipped with either the parallel stator windings or the rotor cage (damper winding). In all these tests, the model performed very well.

It is worth mentioning that the estimated set of force model parameters corresponds to a certain operating point (supply voltage, load torque, etc.) of an electrical machine. Slot harmonics are considered as one of the main reasons for the dependence of the electromagnetic force on the loading. These have a very small whirling frequency dependence in the range considered, but can vary significantly due to the load changes. Moreover, as shown above, the configuration of the stator winding may influence profoundly the shape of FRF of the UMP; therefore, different sets of parameters may have to be used for a machine of the same geometry, but with different stator winding connections.

4.2 Influence of parallel stator windings on the UMP constituents

The rotor eccentricity disturbs the symmetric distribution of the magnetic field in the air gap of the motor by introducing many new magnetic field harmonics. The orders of these harmonics differ by one (±1) from the orders of the harmonics, which already existed in the machine with a concentric rotor. The interaction between these magnetic fields causes the UMP. Of key importance are the harmonics related to the fundamental magnetic field and those associated with slotting, as they constitute the major part of the UMP. Figure 4.6 shows that the UMP due to these two components accounts for ¾ of the total UMP.

In Publication P6, the influence of parallel stator windings on the total UMP and its constituents is studied using the FEA. The results of this study showed that the parallel stator windings effectively attenuate the net eccentricity force by suppressing significantly the eccentricity harmonics related to the fundamental magnetic field. The slotting harmonics are mitigated almost evenly in the whole whirling frequency range studied, although not to such a great degree as the harmonics associated with the fundamental magnetic field. It was shown that the reduction of the harmonics related to the fundamental field and slotting accounts for the major part of the UMP mitigation by the parallel stator windings.

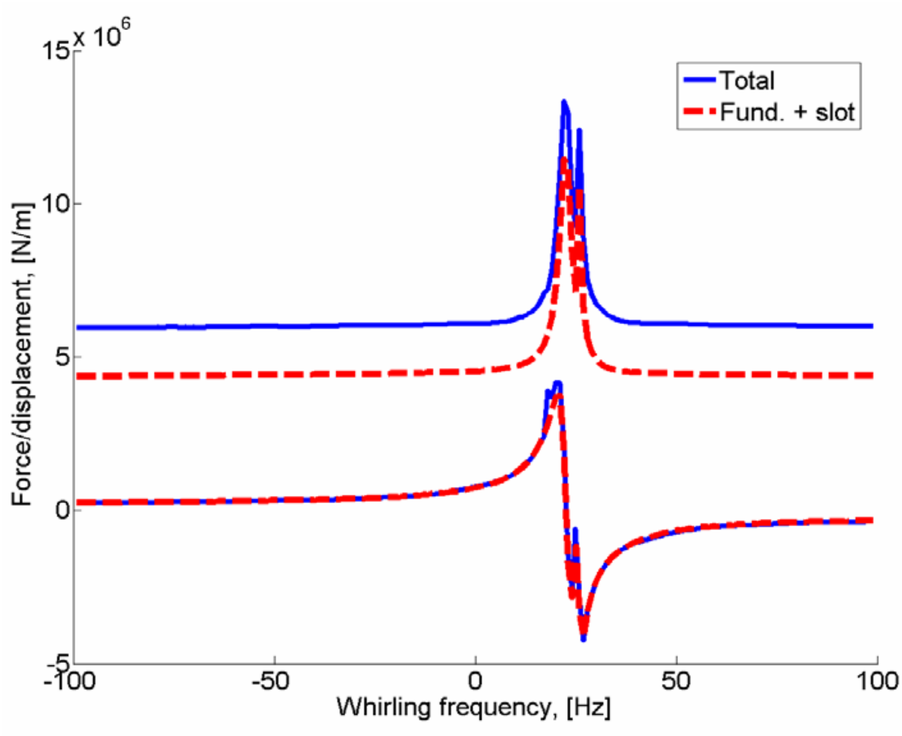

Figure 4.6 Total UMP vs. the sum of two UMP constituents: four-pole, 50 Hz induction motor with rotor cage and series-connected stator windings at the rated load.

4.3 Other issues related to the parallel stator windings

Although, both the parallel stator windings and rotor cage tend to reduce the eccentricity force, their effects on the UMP are still very different. Thus, the rotor cage, containing usually a large number of parallel paths uniformly distributed around the rotor circumference, evenly decreases the UMP magnitude, independently of the rotor-eccentricity phase angle. The stator winding, on the other hand, contains normally fewer parallel paths. Therefore, the degree of the UMP reduction by the stator winding may depend on the position of the rotor axis displacement, causing the electromagnetic system of the motor to behave anisotropically. Moreover, the degree, to which the UMP is affected by the stator winding, may also depend heavily on the number of parallel paths. As seen in Figure 4.7, the trace of the eccentricity force vector in the induction motor containing two parallel paths in the stator winding (2PP) differs significantly from the UMP trace in the same motor with four parallel paths (4PP). Unlike the latter trace, which is almost circular, the former trace has considerably different values on the orthogonal axes. In both cases simulated, the cylindrical circular rotor eccentricity was used, the whirling radius was 20% of the nominal air gap and whirling frequency was –25 Hz.

This anisotropic UMP behaviour causes the results of numerical impulse response test to deviate noticeably from the results of conventional FEM technique (forced whirling method). In Publication P4, the performance of the impulse response test with different combinations of stator and rotor windings layouts is investigated and some conclusions as to the applicability of the method are drawn.

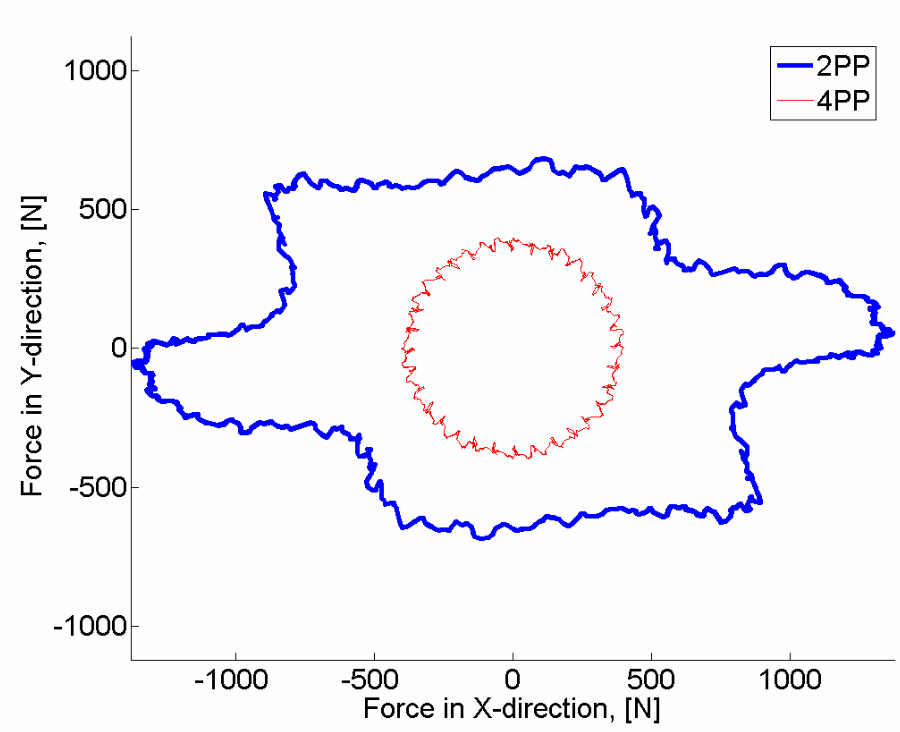

Figure 4.7 Traces of UMP in four-pole, 50 Hz induction motor with parallel stator windings but without rotor cage at no load.

4.4 Parallel stator windings vs. rotor cage vs. parallel stator windings + rotor cage

Parallel connections in the rotor and stator windings have long been known to effectively reduce the UMP. As the rotor cage (damper winding) usually contains many more parallel circuits than the stator winding, it is natural to assume that motors equipped with the rotor cage alone would experience a lower level of eccentricity force than those where only the parallel stator windings are provided. Furthermore, motors with parallel circuits both in the rotor and stator are expected to vibrate less than those with parallel paths either in the rotor or stator.

According to the numerical calculation results presented in Figure 4.8, two parallel stator windings indeed provide weaker UMP mitigation than the rotor cage alone. These findings correspond to a standard 15 kW induction motor at no load. Besides, two parallel stator windings may also cause the uneven UMP mitigation discussed above.

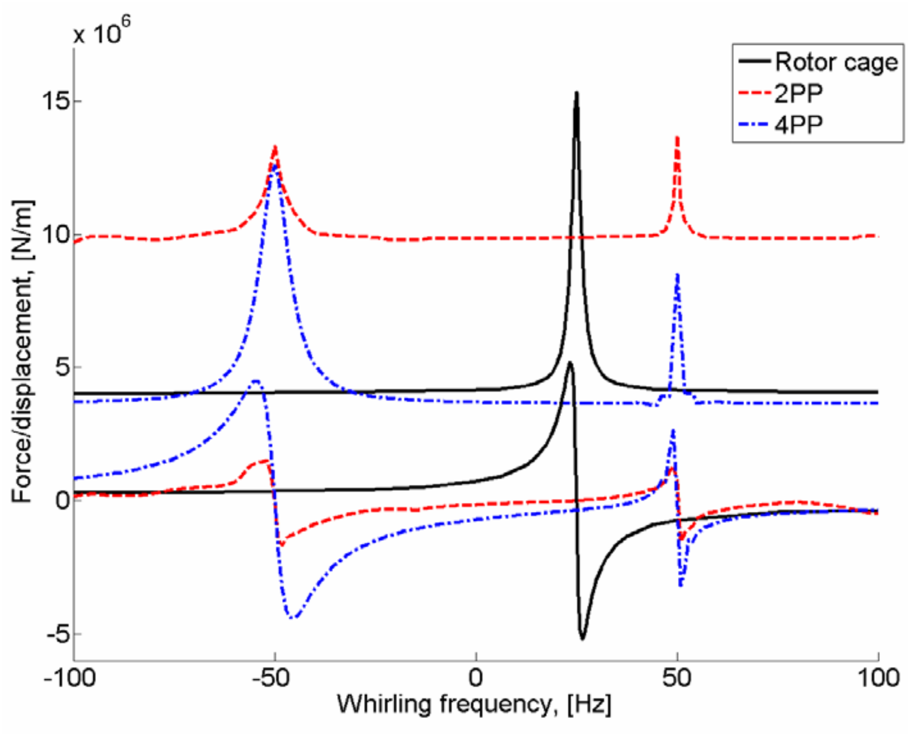

Figure 4.8 Comparison of FRFs of the UMP in four-pole, 50 Hz induction motor at no load.

However, contrary to what was anticipated, an even lower average level of UMP was attained in the whirling frequency range considered when the motor had four parallel stator windings. Similar results were also observed in a salient-pole synchronous machine operated at the rated load. As seen in Figure 4.9, the UMP when four parallel circuits are provided in the stator winding is substantially lower than that in the machine equipped with the damper winding only. These results show that already four parallel stator windings can have a stronger impact on the UMP than the rotor cage (damper winding).

As expected, the smallest eccentricity forces are produced in the motors incorporating parallel circuits both in the rotor and stator (see Figure 4.9).

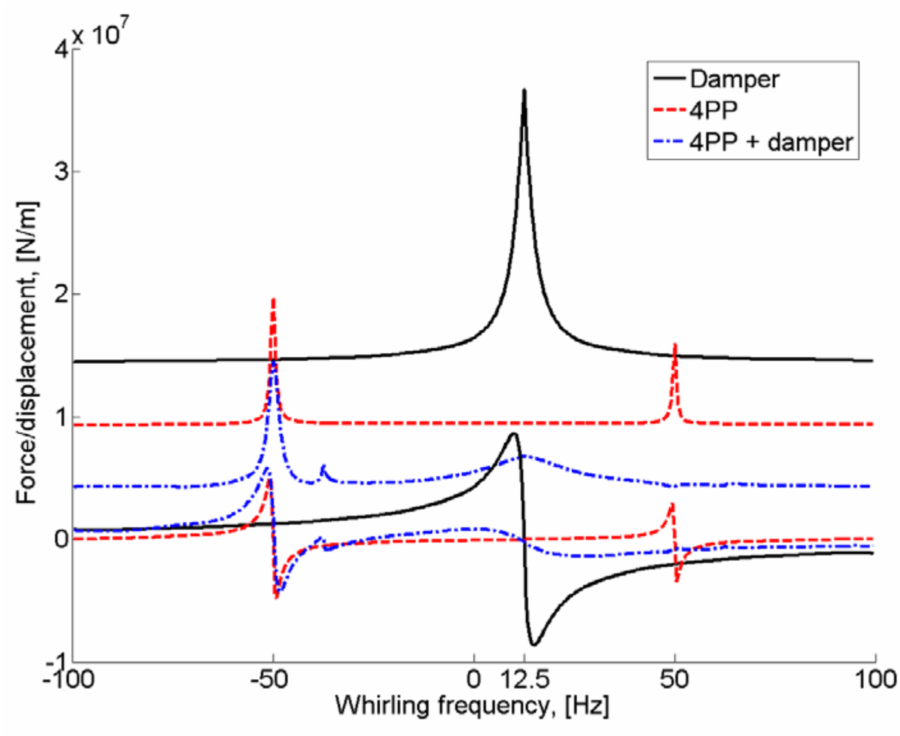

Figure 4.9 Comparison of FRFs of the UMP in eight-pole, 50 Hz salient-pole synchronous generator.

4.5 Conclusions

In this chapter, the main results of the thesis are presented and discussed in brief. The presented parametric force models are verified using the numerical simulations of the test motors. All force models exhibited a very good performance throughout the whole whirling frequency range considered.

In this work, three electrical machines with different combinations of the rotor and stator winding layouts were employed to investigate the performance of the force models developed. In addition to the machines described in Tables 3.1 and 3.2, a six-pole, 50 Hz, 18.5 kW cage induction motor was used. Although the force models performed very well with all these test machines, the applicability of the models to every type of electrical machine cannot be guaranteed. However, these models continue the work started earlier by Arkkio et al. (2000) and Holopainen et al. (2005a) and extend significantly the area of the force models applicability by addressing the following electrical machines:

- salient- and non-salient-pole synchronous machines equipped with damper winding and with series-connected stator windings;

- salient- and non-salient-pole synchronous machines equipped with parallel stator windings and with no damper winding;
- induction motors equipped with parallel stator windings and with no rotor cage (e.g., wound-rotor induction motor, blank-rotor induction motor);
- salient- and non-salient-pole synchronous machines equipped with damper winding and with parallel stator windings;
- induction motors equipped with rotor cage and parallel stator windings.

Interaction between the currents circulating in the parallel circuits of the rotor and stator may influence the UMP and alter the shape of its FRF to some extent. Although being relatively small, the effects of this interaction could still be investigated further in order to improve the accuracy of the parametric force models.

It was shown that the magnetic field harmonics associated with the fundamental magnetic field and slotting contribute the most to the total UMP. The parallel stator windings may considerably suppress these UMP constituents and, hence, reduce the net UMP.

Parallel stator windings were shown to cause anisotropic UMP behaviour, especially in electrical machines without the rotor cage (damper winding). These findings conform well to the results presented by Robinson (1943). The author stated that there is no damping of the UMP along the line between the two parallel stator windings. Due to this UMP anisotropy, care should be exercised when applying the numerical impulse response test to analyse such motors.

Parallel paths in the stator winding may provide a more efficient UMP mitigation than the rotor cage (damper winding), even if the number of parallel circuits in the stator is substantially lower than the number of parallel circuits in the rotor. Using parallel connections in the rotor and stator simultaneously ensures the lowest level of the UMP. The last statement agrees well with the results presented by Arkkio (1996).

The FEA results acquired in this work were not verified by measurements. However, the employed finite-element models and numerical techniques for the electromagnetic force calculation were previously validated by Arkkio et al. (2000), Lantto et al. (2000) and Tenhunen et al. (2003d). The authors studied the electromagnetic forces in a 15 kW induction motor with different types of rotor eccentricity using the technique presented by Coulomb (1983). Antila et al. (1998) used Coulomb’s approach and the method presented by Arkkio to calculate the electromagnetic forces in the radial active magnetic bearings. In all these contributions, the authors reported a very good agreement between the computed and measured results.

The force models developed were only tested with induction motors and a salient-pole synchronous machine. However, the application area of the models could be extended to other types of rotating electrical machines, especially if their construction is similar to the construction of the motors studied in this work. Thus, by equating the term $B_{p,2}$ to zero, the force model described by Eq. (3.1) can straightforwardly be applied to a cylindrical-rotor synchronous machine. In permanent magnet synchronous motors, eccentricity harmonics can induce eddy-currents in the permanent magnets located on the rotor surface. The eddy-currents would reduce the magnetic field asymmetry and the resultant UMP. In this way, the permanent magnets could be viewed as a rotor cage. Thus, the proposed force models could also be applied to these electrical machines.

Although the developed force models were only tested on the electrical machines with cylindrical circular rotor whirling, the models are also anticipated to perform well with other types of rotor eccentricity. According to the results by Tenhunen et al. (2003d), in electrical motor, the rotor motion of which can be described as the combination of symmetric conical whirling and cylindrical circular whirling, the resultant electromagnetic force on the rotor is almost the same as in the case of cylindrical circuit whirling, provided the radii of symmetric conical whirling and cylindrical circular whirling are equal. Thus, the developed force models could also be applied to describe the UMP in electrical motors with such rotor whirling motion.

The rotors of both machines simulated were not skewed. The rotor skewing can significantly affect the voltages induced in the rotor bars by the magnetic field harmonics, especially the voltages induced by the magnetic field harmonics with short wavelengths (e.g., harmonics related to stator and rotor slotting). The voltages induced in the rotor bars by the eccentricity harmonics, which have relatively long wavelengths, remain virtually unaltered by the skewing. Voltages induced in the rotor bars by a certain magnetic field harmonic define the amount of damping of this harmonic produced by the rotor cage. Thus, it is expected that the damping of slot harmonics by the skewed rotor cage can substantially differ from the damping produced by the rotor cage with straight bars. According to the results presented in Publication P6, slot harmonics contribute significantly to the total unbalanced force. However, the UMP component related to slotting has very small whirling frequency dependence, in the whirling frequency range considered. As shown in Publication P6, peaks in the FRF of the electromagnetic force are caused primarily by the eccentricity harmonics. Thus, rotor skewing, by affecting the voltages induced in the rotor bars by the slot harmonics, can alter the average level of the FRF of the electromagnetic force. Yet, the location of the peaks in the FRF of the force and their elevation above the average FRF level are expected to be almost the same as in the machine with straight rotor bars. Therefore, the force models developed are also expected to be applicable to the machines with skewed rotors.

5 Summary

In this thesis, the UMP caused by the eccentric rotor is investigated in a wide whirling frequency range. Two common types of electrical machine are considered: cage induction motor and salient-pole synchronous machine. Special attention is drawn to the effects of parallel stator windings on the UMP.

Simple analytical models describing the UMP are developed and verified using the FEA. The parametric force models are built for: salient-pole synchronous machines without the parallel stator windings; electrical motors with parallel circuits in the stator only; and electrical machines with parallel paths both in the rotor and stator. The two force models mentioned last were applied to the induction and synchronous motors. All the presented models exhibited a very good performance throughout the whole whirling frequency range considered.

Parallel stator windings, similarly to the rotor cage (damper winding), effectively reduce the UMP. Especially the UMP constituents related to the fundamental magnetic field and slotting are strongly affected by the parallel paths in the stator. However, unlike the rotor cage, the parallel stator windings may instigate anisotropy in the UMP. In such cases, the results of the numerical impulse response test may differ significantly from the conventional calculation results.

Despite the fact that the number of parallel circuits in the stator is often substantially lower than the number of parallel circuits in the rotor, the parallel paths in the stator winding may still provide a more efficient UMP mitigation than the rotor cage (damper winding).

When parallel circuits are provided both in the rotor and stator, the smallest amount of the UMP is expected. However, currents circulating in these parallel paths may interact with each other, thus affecting the UMP and the shape of its FRF.

References

Al-Nuaim, N. A., Toliyat, H. A. 1997. A method for dynamic simulation and detection of dynamic air-gap eccentricity in synchronous machines. *Proceedings of the IEEE International Electric Machines and Drives Conference*, Milwaukee, USA, pp. MA2 5.1-5.3.

Al-Nuaim, N. A., Toliyat, H. A. 1998. Novel method for modeling dynamic air-gap eccentricity in synchronous machines based on modified winding function theory. *IEEE Transactions on Energy Conversion*, Vol. 13, No. 2, pp. 156-162.

Antila, M., Lantto, E., Arkkio, A. 1998. Determination of forces and linearised parameters of radial active magnetic bearings by finite element technique. *IEEE Transactions on Magnetics*, Vol. 34, No. 3, pp. 684-694.

Arkkio, A. 1987. Analysis of induction motors based on the numerical solution of the magnetic field and circuit equations. *Acta Polytechnica Scandinavica, Electrical Engineering Series*, No. 59, Helsinki, 97 p. Available at: http://lib.tkk.fi/Diss/. ISBN 951-666-250-1. (Doctoral thesis).

Arkkio, A., Lindgren, O. 1994. Unbalanced magnetic pull in a high-speed induction motor with an eccentric rotor. *Proceedings of the International Conference on Electrical Machines*, September 5-8, 1994, Paris, France, Vol. 1, pp. 53-58.

Arkkio, A. 1996. Unbalanced magnetic pull in cage induction motors – dynamic and static eccentricity. *Proceedings of the International Conference on Electrical Machines*, September 10-12, 1996, Vigo, Spain, pp. 192-197.

Arkkio, A. 1997. Unbalanced magnetic pull in cage induction motors with asymmetry in rotor structures. *Eighth International Conference on Electrical Machines and Drives EMD-97*, Conference Publication No. 444, September 1-3, 1997, pp. 36-40.

Arkkio, A., Antila, M., Pokki, K., Simon, A., Lantto, E. 2000. Electromagnetic force on a whirling cage rotor. *IEE Proceedings – Electric Power Applications*, Vol. 147, No. 5, pp. 353-360.

Bastos, J. P. A., Sadowski, N. 2003. Electromagnetic modeling by finite element methods. Marcel Dekker, New York, 490 p.

Belmans, R., Geysen, W., Jordan, H., Vandenput, A. 1982a. Unbalanced magnetic pull and homopolar flux in three-phase induction motors with eccentric rotors. *Proceedings of ICEM'82*, pp. 916-921.

Belmans, R., Geysen, W., Jordan, H., Vandenput, A. 1982b. Unbalanced magnetic pull in three-phase two-pole motors with eccentric rotor. *Proceedings of International Conference on Electrical Machines – Design and Application*, London, pp. 65-69.

Belmans, R., Vandenput, A., Geysen, W. 1985 .Determination of the parameters of the radial vibrations of large electric motors. *Symposium on Electromechanics and Industrial*

Electronics Applied to Manufacturing Processes, September 17-19, 1985, San Felice Circeo, Italy, pp. 113-119.

Belmans, R., Vandenput, A., Geysen, W. 1987. Calculation of the flux density and the unbalanced pull in two pole induction machines. *Electrical Engineering (Archiv fur Elektrotechnik)*, Vol. 70, No. 3, pp 151-161.

Berman, M. 1993. On the reduction of magnetic pull in induction motors with off-centre rotor. *Conference Record of the IEEE Industry Applications Society Annual Meeting*, October 2-8, 1993, Vol. 1, pp. 343-350.

Binns, K. J., Dye, M. 1973. Identification of principal factors causing unbalanced magnetic pull in cage induction motors, *Proceeding IEE*, Vol. 120, No. 3, pp. 349-354.

Bossio, G., De Angelo, C., Solsona, J., Garcia, G., Valla, M. I. 2004. A 2-d model of the induction machine: an extension of the modified winding function approach. *IEEE Transactions on Energy Conversion*, Vol. 19, No. 1, pp. 144-150.

Cai, W., Pillay, P., Reichert, K. 2001. Accurate computation of electromagnetic forces in switched reluctance motors. *Proceedings of the Fifth International Conference on Electrical Machines and Systems, ICEMS 2001*, August 18-20, 2001, Vol. 2, pp. 1065-1071.

Chari, M. V. K., Silvester, P. P. 1980. Finite elements in electrical and magnetic field problems. J. Wiley & Sons, New York, 219 p.

Chari, M., Konrad, A., Palmo, M., D'Angelo, J. 1982. Three-dimensional vector potential analysis for machine field problems. *IEEE Transactions on Magnetics*, Vol. 18, No. 2, pp. 436-446.

Coulomb, J. L. 1983. A methodology for the determination of global electromechanical quantities from a finite element analysis and its application to the evaluation of magnetic forces, torques and stiffness. *IEEE Transactions on Magnetics*, Vol. 19, No. 6, pp 2514-2519.

Covo, A. 1954. Unbalanced magnetic pull in induction motors with eccentric rotors. *AIEE Transactions*, Vol. 73, pp. 1421-1425.

DeBortoli, M. J., Salon, S. J., Burow, D. W., Slavik, C. J. 1993. Effects of rotor eccentricity and parallel windings on induction machine behaviour: a study using finite element analysis. *IEEE Transactions on Magnetics*, Vol. 29, No. 2, pp. 1676-1682.

Dorrell, D. G. 1993. Calculation of unbalanced magnetic pull in cage induction machines. Cambridge: University of Cambridge. 169 p. (Doctoral thesis).

Dorrell, D. G., Smith, A. C. 1994. Calculation of UMP in induction motors with series or parallel winding connections. *IEEE Transactions on Energy Conversion*, Vol. 9, No. 2, pp. 304-310.

Dorrell, D. G. 1995a. The influence of rotor skew on unbalanced magnetic pull in cage induction motors with eccentric rotors. *Seventh International Conference on Electrical Machines and Drives*, September 11-13, 1995, Conference Publication No. 412, pp. 67-71.

Dorrell, D. G. 1995b. The sources and characteristics of unbalanced magnetic pull in cage induction motors with either static or dynamic rotor eccentricity. *Proceedings of Stockholm Power Tech*, June 18-22, 1995, Stockholm, Sweden. Vol. Electrical Machines and Drives, pp. 229-234.

Dorrell, D. G. 1996. Calculation of unbalanced magnetic pull in small cage induction motors with skewed rotors and dynamic rotor eccentricity. *IEEE Transactions on Energy Conversion*, Vol. 11, No. 3, pp. 483-488.

Dorrell, D. G. 1999. Experimental behaviour of unbalanced magnetic pull in 3-phase induction motors with eccentric rotors and the relationship with tooth saturation. *IEEE Transactions on Energy Conversion*, Vol. 14, No. 3, pp. 304-309.

Dorrell, D. G. 2000. Modelling of non-uniform rotor eccentricity and calculation of unbalanced magnetic pull in a 3-phase cage induction motors. *Proceeding of ICEM 2000*, August 28-30, 2000, Espoo, Finland, pp. 1820-1824.

Dorrell, D. G., Ooshima, M., Chiba, A. 2003. Force analysis of a buried permanent-magnet bearingless motor. *IEEE International Electric Machines and Drives Conference, IEMDC 2003*, June 1-4, 2003, Vol. 2, pp. 1091-1097.

Ellison, A. J., Moore, C. J. 1968. Acoustic noise and vibration of rotating electric machines. *IEE Proceedings*, Vol. 115, No. 11, pp. 1633-1640.

Felippa, C. A. 2001. A historical outline of matrix structural analysis: a play in three acts. *Computers and Structures*, Vol. 79, No. 14, pp. 1313-1324.

Fisher-Hinnen, J. 1899. Dynamo design. Van Nostrand.

Freise, W., Jordan, H. 1962. Unbalanced magnetic pull in 3-phase a.c. machines. *ETZ-A*, Vol. 83, No. 9, pp. 299-303; Translation: CE Trans. 7836.

Frohne, H. 1967. The practical importance of unbalanced magnetic pull, possibilities of calculating and damping it. *Conti Elektro Berichte*, Vol. 13, pp. 81-92. Translation: ERA Transactions 1B2617.

Fruchtenicht, J., Jordan, H., Seinsch, H. O. 1982. Exzentrizitätsfelder als Ursache von Lafinstabilitäten bei Asynchronmaschinen. Teil I und II. *Archiv fur Elektrotechnik*, Vol. 65, pp. 271-292.

Garrigan, N. R., Soong, W. L., Stephens, C. M., Storace, A., Lipo, T. A. 1999. Radial force characteristics of a switched reluctance machine. *Industry Applications Conference, Thirty-fourth IAS Annual Meeting*, October 3-7, 1999, Vol. 4, pp. 2250-2258.

Gray, A., Pertsch, J. G. 1918. Critical review of the bibliography on unbalanced magnetic pull in dynamo-electric machines. *AIEE Transactions*, Vol. 37, Part 2, pp. 1417-1424.

Haase, H., Jordan, H., Kovacs, K. P. 1972. Vibratory forces as a result of shaft fluxes with two-pole induction machines. *Electrotech. (ETZ)*, Vol. 93, pp. 485-486. Translation: CEGB CE 7822.

Heller, B., Jokl, A. L. 1969. Tangential forces in squirrel-cage induction motors. *IEEE Transactions on Power Apparatus and Systems*, Vol. 88, No. 4, pp. 484-492.

Hellmund, R. E. 1907. Series versus parallel windings for a.c. motors. *Electrical World*, No. 49, pp. 388-389.

Holopainen, T. P. 2004. Electromechanical interaction in rotordynamics of cage induction motors. Espoo: VTT Technical Research Centre of Finland, VTT Publications 543, 64 p. Available at: http://lib.tkk.fi/Diss/. ISBN 951-38-6404-9. (Doctoral thesis).

Holopainen, T. P., Tenhunen, A., Lantto, E., Arkkio, A. 2005a. Unbalanced magnetic pull induced by arbitrary eccentric motion of cage rotor in transient operation. Part 1: Analytical model. *Electrical Engineering (Archiv fur Elektrotechnik)*, Vol. 88, No. 1, pp. 13-24.

Holopainen, T. P., Tenhunen, A., Lantto, E., Arkkio, A. 2005b. Unbalanced magnetic pull induced by arbitrary eccentric motion of cage rotor in transient operation. Part 2: Verification and numerical parameter estimation. *Electrical Engineering (Archiv fur Elektrotechnik)*, Vol. 88, No. 1, pp. 25-34.

Joksimovic, G. M., Durovic, M. D., Obradovic, A. B. 1999. Skew and linear rise of MMF across slot modeling – winding function approach. *IEEE Transactions on Energy Conversion*, Vol. 14, No. 3, pp. 315-320.

Joksimovic, G. M., Penman, J. 2000. The detection of inter-turn short circuits in the stator windings of operating motors. *IEEE Transactions on Industrial Electronics*, Vol. 47, No. 5, pp. 1078-1084.

Joksimovic, G. M., Durovic, M. D., Penman, J., Arthur, N. 2000. Dynamic Simulation of Dynamic Eccentricity in Induction Machines – Winding Function Approach. *IEEE Transactions on Energy Conversion*, Vol. 15, No. 2, pp. 143-148.

Jordan, H., Roder, G., Weis, M. 1967. Under what circumstances may mechanical vibrations of the stator core be expected at supply frequency in four-pole three-phase asynchronous machines? *Elecktrie*, Vol. 21, No. 3, pp. 91-95; Translation: ERA Trans. 1B2578.

von Kaehne, P. 1963. Unbalanced magnetic pull in rotating electrical machines. Survey of published work. ERA Report, ref.: Z/T 142, 1963, 30 p.

Kim, U., Lieu, D. K. 1998. Magnetic field calculation in permanent magnet motors with rotor eccentricity: without slotting effect. *IEEE Transactions on Magnetics*, Vol. 34, No. 4, Part 2, pp. 2243-2252.

Kovacs, K. P. 1977. Two-pole induction-motor vibrations caused by homopolar alternating fluxes. *IEEE Transactions on Power Apparatus and Systems*, Vol. PAS-96, No. 4, pp. 1105-1108.

Krondl, M. 1956. Self excited radial vibrations of the rotor of induction machines with parallel paths in the winding. *Bull. Assoc. Suisse. Elect.*, Vol. 47, pp. 581-588.

Kyung-Tae Kim; Kwang-Suk Kim; Sang-Moon Hwang; Tae-Jong Kim; Yoong-Ho Jung. 2001. Comparison of magnetic forces for IPM and SPM motor with rotor eccentricity. *IEEE Transactions on Magnetics*, Vol. 37, No. 5, Part 1, pp. 3448-3451.

Lantto, E., Arkkio, A., Antila, M., Pokki, K., Simon, A. 2000. Electromagnetic forces caused by cage induction motor. *7-th International Symposium on Magnetic Bearings*, August 23-25, 2000, ETH Zurich, pp. 589-594.

Li, J. T., Liu, Z. J., Nay, L. H. 2007. Effect of radial magnetic forces in permanent magnet motors with rotor eccentricity. *IEEE Transactions on Magnetics*, Vol. 43, No. 6, pp. 2525-2527.

Lipo, T. A. 1987. Theory and control of synchronous machines. University of Winconsin-Madison.

Lundstrom, L., Gustavsson, R., Aidanpaa, J.-O., Dahlback, N., Leijon, M. 2007. Influence on the stability of generator rotors due to radial and tangential magnetic pull force. *IET Electric Power Applications*, Volume. 1, No. 1, pp. 1-8.

Luo, X., Liao, Y., Toliyat, H. A., El-Antably, A., Lipo, T. A. 1995. Multiple coupled circuit modeling of induction machines. *IEEE Transactions on Industry Applications*, Vol. 31, No. 2, pp. 311-318.

Luomi, J. 1993. Finite element methods for electrical machines. Lecture notes for a postgraduate course in electrical machines. Chalmers University of Technology, Department of Electrical Machines and Power Electronics, Göteborg.

Martin, H. C., Carey G. F. 1973 . Introduction to finite element analysis – Theory and applications. McGraw-Hill Publ., New York, 386 p. ISBN 0-07-040641-3.

Milimonfared, J., Kelk, H. M., Nandi, S., Minassians, A. D., Toliyat, H. A. 1999. A novel approach for broken-rotor-bar detection in cage induction motors. *IEEE Transactions on Industry Applications*, Vol. 35, No. 5, pp. 1000-1006.

Mizia, J., Adamiak, K., Eastham, A. R., Dawson, G. E. 1988. Finite element force calculation: Comparison of methods for electric machines. *IEEE Transactions on Magnetics*, Vol. 24, No. 1, pp. 447-450.

Nandi, S., Toliyat, H. A., Parlos, A. G. 1997. Performance analysis of a single phase induction motor under eccentric conditions. *IEEE Industry Applications Society, Annual Meeting*, October 5-9, 1997, New Orleans, Louisiana, USA, pp. 174-181.

Nandi, S., Bharadwaj, R. M., Toliyat, H. A., Parlos, A. G. 1998. Performance analysis of a three phase induction motor under mixed eccentricity condition. *Proceeding of*

International Conference on Power Electronic Drives and Energy Systems for Industrial Grows, Vol. 1, December 1-3, 1998, pp. 123-128.

Nandi, S., Ahmed, S., Toliyat, H. A. 2001. Detection of rotor slot and other eccentricity related harmonics in a three phase induction motor with different rotor cages. *IEEE Transactions on Energy Conversion*, Vol. 16, No. 3, pp. 253-260.

Nandi, S., Toliyat, H. A. 2002. Novel frequency-domain-based technique to detect stator interturn faults in induction machines using stator-induced voltages after switch-off. *IEEE Transactions on Industry Applications*, Vol. 38, No. 1, pp. 101-109.

Neves, C. G. C., Carlson, R., Sadowski, N., Bastos, J. P. A., Soeiro, N. S., Gerges, S. N. Y. 1998. Vibrational behavior of switched reluctance motors by simulation and experimental procedures. *IEEE Transactions on Energy Conversion*, Vol. 34, No. 5, pp. 3158-3161.

Perers, R., Lundin, U., Leijon, M. 2007. Saturation effects on unbalanced magnetic pull in a hydroelectric generator with an eccentric rotor. *IEEE Transactions on Magnetics*, Vol. 43, No. 10, pp 3884-3890.

Reichert, K., Freundl, H., Vogt, W. 1976. The calculation of forces and torques within numerical magnetic field calculation methods. *Compumag conference*, Oxford 1976, pp. 64-73.

Robinson, R. C. 1943. The calculation of unbalanced magnetic pull in synchronous and induction motors. *AIEE Transactions*, Vol. 62, pp. 620-624.

Robinson, R. C. 1963. Line frequency magnetic vibrations of A.C. machines. *AIEE Transactions on Power Apparatus and Systems*, Vol. 81, pp. 675-679.

Rosenberg, E. 1918. Magnetic pull in electric machines. *Transactions of the American Institute of Electrical Engineers (AIEE)*, Vol. 37, Part 2, New York, N.Y., USA, pp. 1425-1469.

Sadowski, N., Lefevre, Y., Lajoie-Mazenc, M., Cros, J. 1992. Finite element torque calculation in electrical machines while considering the movement. *IEEE Transactions on Magnetics*, Vol. 28, No. 2, pp. 1410-1413.

Salon, S. J., DeBortoli, M. J., Burow, D. W., Slavik, C. J. 1992. Calculation of circulating current between parallel windings in induction motors with eccentric rotors by finite element method. *International Conference on Electrical Machines*, September 15-17, 1992, Manchester, UK, pp. 371-375.

Salon, S., Sivasubramaniam, K., Ergene, L. T. 2001. The effect of asymmetry on torque in permanent magnet motors. *IEEE International Electric Machines and Drives Conference, IEMDC 2001*, pp. 208-217.

Schlensok, C., Henneberger, G. 2004. Calculation of force excitations in induction machines with centric and excentric positioned rotor using 2-d transient FEM. *IEEE Transactions on Magnetics*, Vol. 40, No. 2, pp. 782-785.

Schuisky, V. W. 1971. Magnetic pull in electrical machines due to eccentricity of the rotor. *Electrotech. Masch. Ball*, Vol. 88, pp. 391-399. Translation: ERA 2958.

Silvester, P. P., Ferrari, R. L. 1996. Finite elements for electrical engineers. Third Edition, Cambridge University Press, 512 p.

Smith, A. C., Dorrell, D. G. 1996. Calculation and measurement of unbalanced magnetic pull in cage induction motors with eccentric rotors. Part 1: Analytical model. *IEE Proceedings – Electric Power Applications*, Vol. 143, No. 3, pp. 193-201.

Stavrou, A., Penman, J. 2001. Modelling dynamic eccentricity in smooth air-gap induction machines. *IEEE International Electric Machines and Drives Conference, IEMDC 2001*, pp. 864-871.

Summers, E. W. 1955. Vibration in 2-pole induction motors related to slip frequency. *AIIE Transactions*, Vol. 74, pp. 69-72.

Swann, S. A. 1963. Effect of rotor eccentricity on the magnetic field in the air-gap of a non-salient-pole machine. *IEE Proceedings*, Vol. 110, No. 5, pp. 903-915.

Tarnhuvud, T., Reichert, K. 1988. Accuracy problems of force and torque calculation in FE-systems. *IEEE Transactions on Magnetics*, Vol. 24, No. 1, pp. 443-446.

Tenhunen, A. 2001. Finite-element calculation of unbalanced magnetic pull and circulating current between parallel windings in induction motor with non-uniform eccentric rotor. *Proceedings of Electromotion'01*, June 19-20, 2001, Bologna, Italy, pp. 19-24. Available at: http://lib.tkk.fi/Diss/2003/isbn9512266830/.

Tenhunen, A. 2003. Electromagnetic forces acting between the stator and eccentric cage rotor. Espoo: Helsinki University of Technology. (Laboratory of Electromechanics, Report series No. 69, 40 p.). Available at: http://lib.tkk.fi/Diss/. ISBN 951-22-6682-2. (Doctoral thesis).

Tenhunen, A. 2005. Calculation of eccentricity harmonics of the air-gap flux density in induction machines by impulse method. *IEEE Transactions on Magnetics*, Vol. 41, No. 5, pp. 1904-1907.

Tenhunen, A., Holopainen, T. P., Arkkio, A. 2003a. Impulse method to calculate the frequency response of the electromagnetic forces on whirling cage rotors. *IEE Proceedings – Electric Power Applications*, Vol. 150, No. 6, pp. 752-756.

Tenhunen, A., Holopainen, T. P., Arkkio, A. 2003b. Effects of equalizing currents on electromagnetic forces of whirling cage rotor. *The IEEE International Electric Machines and Drives Conference IEMDC'03*, June 1-4, 2003, Vol. 1, pp. 257-263.

Tenhunen, A., Benedetti, T., Holopainen, T. P., Arkkio, A. 2003c. Electromagnetic forces in cage induction motors with rotor eccentricity. *The IEEE International Electric Machines and Drives Conference IEMDC'03*, June 1-4, 2003, Vol. 3, pp. 1616-1622.

Tenhunen, A., Benedetti, T., Holopainen, T. P., Arkkio, A. 2003d. Electromagnetic forces of the cage rotor in conical whirling motion. *IEE Proceedings - Electric Power Applications,* Vol. 150, No. 5, pp. 563-568.

Tenhunen, A., Holopainen, T. P., Arkkio, A. 2004. Effects of saturation on the forces in induction motors with whirling cage rotor. *IEEE Transactions on Magnetics*, Vol. 40, No. 2, pp. 766-769.

Timar, P. L. 1989. Noise and vibration of electrical machines. Elsevier Science Publishers, Amsterdam – Oxford – New York – Tokyo, 339 p., ISBN 0-444-98896-3.

Toliyat, H. A., Al-Nuaim, N. A. 1997. Simulation and detection of dynamic air-gap eccentricity in salient pole synchronous machine. *IEEE Industry Applications Society Annual Meeting*, October 5-9, 1997, New Orleans, USA, pp. 255-262.

Toliyat, H. A., Lipo, T. A. 1995. Transient analysis of cage induction machines under stator, rotor bar and end ring faults. *IEEE Transactions on Energy Conversion*, Vol. 10, No. 2, pp. 241-247.

Vandevelde, L., Melkebeek, J. A. A. 1994. Theoretical and experimental study of radial forces in relation to magnetic noise of induction motors. *International Conference on Electrical Machines ICEM-1994*, 3, pp. 419-424.

Wignall, A. N., Gilbert, A. J., Yang, S. J. 1988. Calculation of forces on magnetised ferrous cores using the Maxwell stress method. *IEEE Transactions on Magnetics*, Vol. 24, No. 1, pp. 459-462.

Williamson, S. 1983. Power factor improvement in cage rotor induction motors. *IEE Proceedings – Electric Power Applications*, Vol. 130, No. 2, Part B, pp. 121-129.

Williamson, S., Smith, A. C. 1982. Steady-state analysis of 3-phase cage motors with rotor-bar and end-ring faults. *IEE Proceedings – Electric Power Applications*, Vol. 129, No. 3, Part B, pp. 93-100.

Williamson, S., Mirzoian, K. 1985. Analysis of cage induction motors with stator winding faults. *IEEE Transactions on Power Apparatus and Systems*, Vol. PAS-104, No. 7, pp. 1838-1842.

Williamson, S., Abdel-Magied, M. A. S. 1987. Steady-state analysis of double-cage induction motors with rotor-cage faults. *IEE Proceedings – Electric Power Applications*, Vol. 134, No. 4, Part B, pp. 199-206.

Williamson, S., Adams, N. K. 1989. Cage induction motors with inter-rings. *IEE Proceedings – Electric Power Applications*, Vol. 136, No. 6, Part B, pp. 263-274.

Yang, S. J. 1975. Acoustic noise from small 2-pole single-phase induction machines. *Proceeding IEE*, Vol. 122, pp. 1391-1396.

Zhu, Z. Q., Howe, D. 1997. Effect of rotor eccentricity and magnetic circuit saturation on acoustic noise and vibration of single-phase induction motors. *Electric Machines and Power Systems*, Vol. 25, pp. 443-457.

ISBN 978-951-22-9005-5
ISBN 978-951-22-9006-2 (PDF)
ISSN 1795-2239
ISSN 1795-4584 (PDF)